TABLE 1—(*Continued*)

| JCI No | Name | Abbreviation | Application/Target/Mechanism |
|---|---|---|---|
| −418 | Acrylamide | | Neurotoxin/carcinogenicity |
| −417 | Hexachlorobenzene | BHC | Agricultural chemical/carcinogenicity |
| −346 | 2-Deoxyglucose | 2-DG | Glycolytic pathway/glycosylation inhibitor |
| −325 | Pentachlorophenol | PCP | Agricultural chemical/teratogenicity/carcinogenicity |
| −324 | Aniline | | Oxidative stress/methemoglobinemia/carcinogenicity |
| −323 | Triazine | | Agricultural chemical |
| −322 | Edifenphos | EDDP | Agricultural chemical/antibiotics/choline esterase |
| −321 | γ-1,2,3,4,5,6-Hexachlorocyclohexane | γ-BHC | Agricultural chemical/carcinogenicity |
| −320 | Dichlorvos | DDVP | Agricultural chemical/teratogenicity/carcinogenicity |
| −319 | *O*-Ethyl *O*-4-nitrophenyl phenylphosphonothioate | EPN | Agricultural chemical |
| −318 | Cadmium chloride | $CdCl_2$ | Teratogenicity/carcinogenicity |
| −317 | Phenylmercury acetate | PMA | Fungicides/mutagenicity |
| −316 | Mercaptoacetic acid | | Synthetic intermediate |
| −315 | 1,3-Diphenylguanidine | DPG | Vulcanizing agent |
| −314 | 3,4,4′-Trichlorocarbanilide | TCC | Cosmetics/antibacterial agent |
| −313 | 3-Iodo-2-propynyl butylcarbamate | IPBC | Antibacterial agent |
| −311 | 2,3,3,3−2′,3′,3′,3′-Octachlorodipropylether | S-421 | Agricultural chemical/antibacterial agent |
| −310 | 1,2-Benzisothiazolin-3-one | BIT | Antibacterial agent |
| −309 | Isobornylthiocyanoacetate | IBTA | Antibacterial agent |
| −308 | *p*-Chlorophenyl-3-iodopropargylformal | CPIP | Antibacterial agent |
| −307 | Zinc butylxanthate | ZBX | Vulcanizing agent |
| −306 | Polypropylene glycol | PG | Synthetic intermediate |
| −305 | 10,10′-Oxy-bis(phenoxyarsine) | OBPA | Antibacterial agent |
| −296 | Snake venom from *Naja naja kaouthia* | SV-NNK | Snake venom |
| −295 | Snake venom from *Naja nigricollis* | SV-NN | Snake venom |
| −294 | 2,5-di(*tert*-butyl)-1,4-Hydroquinone | DTBHQ | Oxidative stress |
| −293 | Ibotenic Acid | | Mushroom toxin/neurotoxin |
| −292 | *N*-Methy-4-phenyl-1,2,3,6-tetrahydropyridine | MPTP | Neurotoxin |
| −289 | Tetrodotoxin | | Natural product/$Na^+$ channel inhibitor |
| −288 | ICI 182,780 | | Estrogen antagonist |
| −275 | Benzophenone | | Agricultural chemical |
| −274 | 1,2-Dibromo-3-chloropropane | DBCP | Antibacterial agent/insecticide/carcinogenicity |
| −273 | Zineb | | Agricultural chemical |
| −272 | Dieldrin | | Insecticide |
| −271 | Hexachlorobenzene | HCB | Antibacterial agent/carcinogenicity |
| −270 | Ziram | | Antibacterial agent/vulcanizing agent |
| −269 | Chlordane | | Insecticide/carcinogenicity |
| −268 | 4,4′-Dichlorodiphenyltrichloroethane | p,p′-DDT | Insecticide/carcinogenicity/teratogenicity |
| −267 | Bisphenol A | BPA | Estrogenic |
| −266 | 17-β-Estradiol | E2 | Estrogenic |
| −265 | Diethylstilbestrol | DES | Estrogenic |
| −261 | Paraquat | | Agricultural chemical/oxidative stress |
| −247 | Ouabain | | Cardiac glycosides |
| −245 | Okadaic acid | | Natural product/PP1, PP2A inhibitor |
| −242 | Antimycin A1 | | Agricultural chemical |
| −232 | Digoxin | | Cardiac glycosides |
| −201 | OH-Flutamide | | Flutamide derivative/androgen antagonist |
| −200 | Flutamide | | Anticancer drugs/androgen antagonist |
| −185 | 30% $H_2O_2$ | | Oxidative stress |
| −182 | *N*-Acetyl-L-cysteine | NAC | Super oxyside scavenger |
| −181 | L-Ascorbic acid | | Food constituent |
| −179 | Dopamine | | Neurotransmitter |
| −177 | Caffeine | | Food constituent |
| −168 | Cycloheximide | | Protein synthesis inhibitor |
| −144 | 4-Hydroxyphenylretinamide | 4-HPR | RAR |
| −137 | Indomethacin | | COX inhibitor |
| −99 | SN-38 | | Irinotecan derivative/Topo I |
| −96 | Toremifene | | Anticancer drugs/estrogen antagonist |
| −95 | Tamoxifen | | Anticancer drugs/estrogen antagonist |
| −63 | Cyclosporin A | | Anticancer drugs/helper T cell |
| −46 | HCFU | | Anticancer drugs/antimetabolite(pyrimidine) |
| −36 | Docetaxel | | Anticancer drugs/tubulin |
| −35 | Paclitaxel | | Anticancer drugs/tubulin |
| −34 | Colchicine | | Antipodagric/tubulin |
| −33 | Cisplatin | | Anticancer drugs/DNA cross linker |
| −32 | Carboplatin | | Anticancer drugs/DNA cross linker |
| −31 | Irinotecan | | Anticancer drugs/Topo I |
| −30 | Camptothecin | CPT | Anticancer drugs/Topo I |
| −24 | Methotrexate | | Anticancer drugs/DHFR |
| −19 | Vincristine | | Anticancer drugs/tubulin |
| −18 | Vinblastine | | Anticancer drugs/tubulin |
| −16 | Mitomycin-C | MMC | Anticancer drugs/DNA alkylator |
| −9 | Tegafur | | Anticancer drugs/antimetabolite(pyrimidine) |
| −8 | 5-Fluorouracil | 5-FU | Anticancer drugs/antimetabolite(pyrimidine) |
| −5 | Cytarabine | | Anticancer drugs/antimetabolite(pyrimidine) |
| −4 | Nitrogen mustard | | Anticancer drugs/DNA alkylator |

RAR, retinoic acid receptor; RXR; retinoid X receptor.

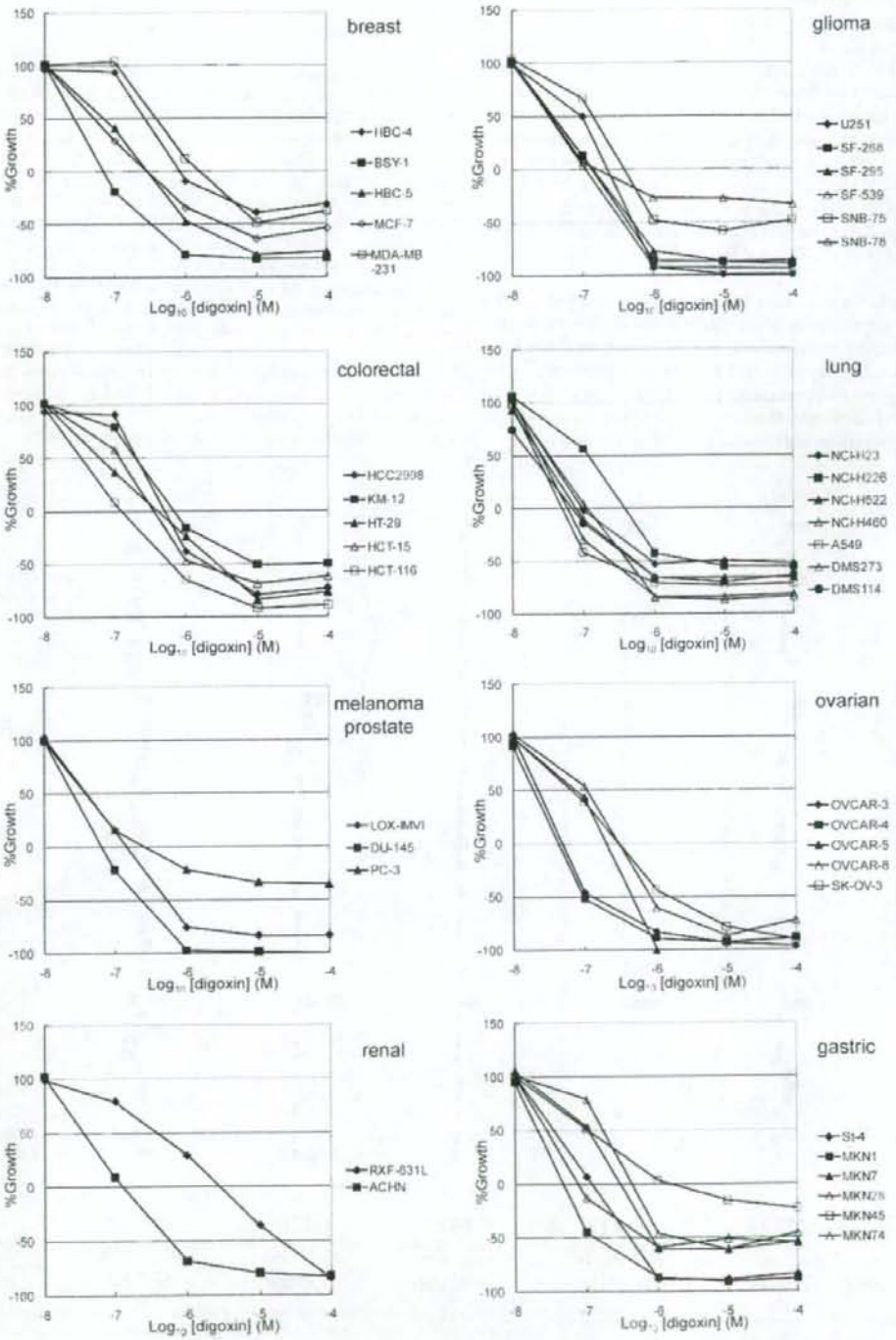


**Fig. 1.** Dose response curves of digoxin against growth of JFCR-39 cells. The *x*-axis represents concentration of digoxin and the *y-axis* represents percentage growth. The GI50 represents the concentration required to inhibit cell growth by 50% compared with untreated controls.

the standard anticancer drugs using the COMPARE algorithm (Yamori et al., 1999). We have used this system successfully and demonstrated that the molecular targets of the novel chemicals MS-274, FJ5002, and ZSTK474 were topoisomerases I and II (Yamori et al., 1999), telomerase (Naasani et al., 1999), and phosphatidylinositol 3-kinase (Yaguchi et al., 2006), respectively. Several other interesting studies, based on a panel of cancer cells, classified anticancer drugs according to their action mechanisms or molecular targets by cluster analysis of their GI50 values (Weinstein et al., 1992, 1997; Dan et al., 2002). Correlation analysis has also been used to explore the genes associated with the sensitivity of the cells in the panel to anticancer drugs (Scherf et al., 2000; Okutsu et al., 2002; Zembutsu et al., 2002; Nakatsu et al., 2005).

In this study, we have examined the potential of the JFCR39 system in classifying various chemicals, and predicted their action mechanisms. For this purpose, we have determined the fingerprints of 130 different types of chemicals including toxic chemicals, pesticides, drugs and synthetic intermediates, and then classified these chemicals according to the cluster analysis of their fingerprints.

## Materials and Methods

**Cell Lines and Cell Cultures.** The panel of human cancer cell lines has been described previously (Yamori et al., 1999; Dan et al., 2002) and consists of the following 39 human cancer cell lines: lung cancer, NCI-H23, NCI-H226, NCI-H522, NCI-H460, A549, DMS273, and DMS114; colorectal cancer, HCC-2998, KM-12, HT-29, HCT-15, and HCT-116; gastric cancer, MKN-1, MKN-7, MKN-28, MKN-45, MKN-74, and St-4; ovarian cancer, OVCAR-3, OVCAR-4, OVCAR-5, OVCAR-8, and SK-OV-3; breast cancer, BSY-1, HBC-4, HBC-5, MDA-MB-231, and MCF-7; renal cancer, RXF-631L and ACHN; melanoma, LOX-IMVI; glioma, U251, SF-295, SF-539, SF-268, SNB-75, and SNB-78; and prostate cancer, DU-145 and PC-3. All cell lines were cultured in RPMI 1640 medium (Nissui Pharmaceutical, Tokyo, Japan) with 5% fetal bovine serum, penicillin (100 units/ml), and streptomycin (100 $\mu$g/ml) at 37°C under 5% $CO_2$.

**Determination of Cell Growth Inhibition Profiles.** Growth inhibition experiments were performed to assess the sensitivity of the cells to various chemicals as described before (Yamori et al., 1999; Dan et al., 2002). Growth inhibition was measured by determining the changes in the amounts of total cellular protein after 48 h of chemical treatment using a sulforhodamine B assay. For each chemical, the growth assay was performed using a total of five different concentrations of the chemical (for example, $10^{-4}$, $10^{-5}$,

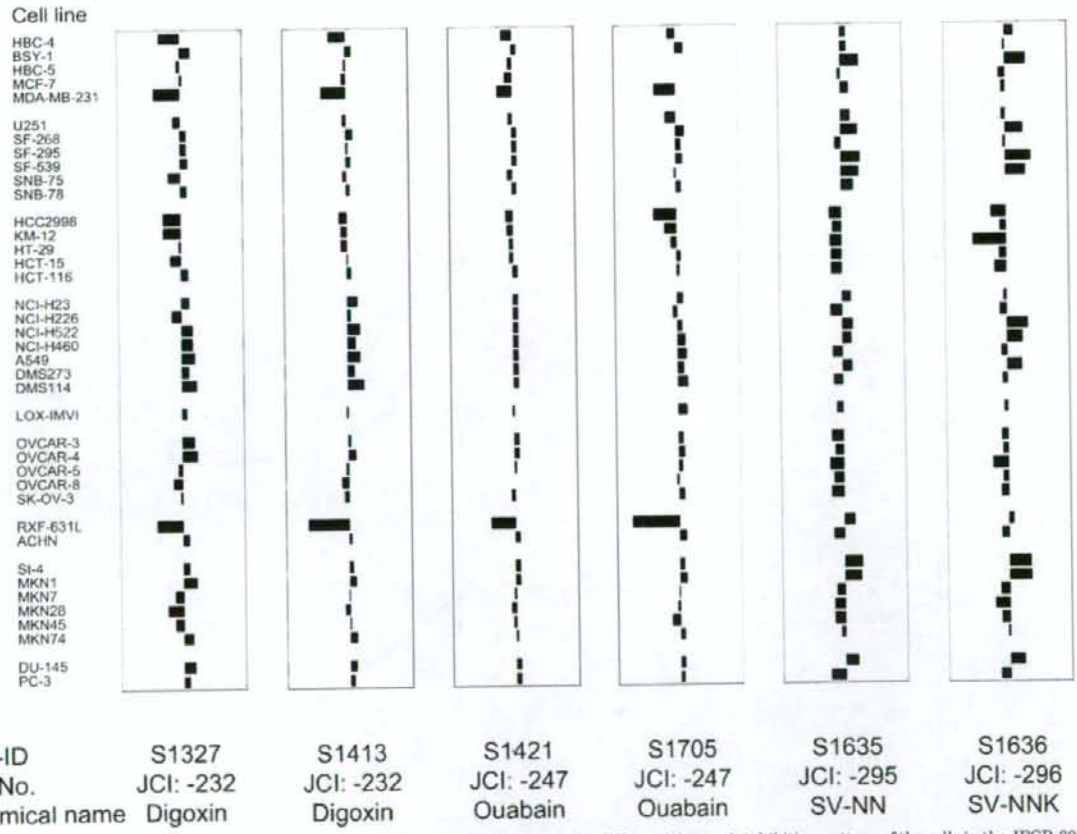


**Fig. 2.** Fingerprints of digoxin, ouabain, SV-NN, and SV-NNK. Fingerprint shows the differential growth inhibition pattern of the cells in the JFCR-39 panel against the test chemical. The *X*-axis represents relative value of GI50; $(-1) \times (\log GI50 - MG\text{-}MID)$; MG-MID is the mean value of the log GI50. Zero means the mean GI50 and one means the GI50 value is 10-fold more sensitive than the mean GI50. Exp-ID and JCI numbers are the ID for the experiment and ID for the chemical, respectively, in our database.

$10^{-6}$, $10^{-7}$, and $10^{-8}$ M) and one negative control. All assays were performed in duplicate. This GI50 calculation method is well established and reliable through anticancer drug screen using NCI60 as well as JFCR39 (Paull et al., 1989; Yamori et al., 1999; Yamori, 2003). At each test concentration, the percentage growth was calculated using the following seven absorbance measurements: growth at time 0 (T0), growth of the control cells (C), and test growth in the presence of five different concentrations (T) of a drug. The percentage growth inhibition was calculated as: % growth = $100 \times [(T - T0)/(C - T0)]$ when $T \geq T0$, and % growth = $100 \times [(T - T0)/T]$ when $T < T0$. The GI50 values, which represent 50% growth inhibition concentration, were calculated as $100 \times [(T - T0)/(C - T0)] = 50$. When the GI50 of a chemical could not be calculated, the highest used concentration was assigned as its GI50 value. Absolute values of GI50 were then log transformed for further analysis. We certified the accuracy of measured GI50 data by using reference control chemicals, such as mitomycin-C, paclitaxel, and SN-38, in every experiment and by checking the dose response curves.

**Chemicals.** Spironolactone, *para*-aminoazobenzene, *para*-cresidine, neostigmine bromide, *para*-dichlorobenzene, phenytoin, *ortho*-toluidine, imipramine, cobalt chloride, atrazine, propylthiouracil, D,L-thalidomide, carbon tetrachloride, hydroquinone, monocrotaline, vinyl chloride, tributyl-tin chloride, valproic acid, benzene, acrylamide, pentachlorophenol, aniline, 1,3-diphenylguanidine, polypropylene glycol, 10,10′-oxy-bis(phenoxyarsine), testosterone propionate, carbaryl, acephate, bisphenol A, 17-$\beta$-estradiol, diethylstilbestrol, and $\alpha$-bungarotoxin were purchased from Wako (Tokyo, Japan). Snake venoms from *Agkistrodon halys blomhoffii*, *Trimeresurus flavoviridis*, *Crotalus atrox*, *Naja nigricollis*, and *Naja naja kaouthia* were purchased from Latoxan (Valence, France). 2-Aminomethylpyridine, 1*H*-1,2,4-triazole, 1*H*-1,2,3-triazole, 3,4,4′-trichlorocarbanilide, edifenphos, dichlorvos, *O*-ethyl *O*-4-nitrophenyl phenylphosphonothioate, 2,4-dinitrophenol, *N*-methylaniline, 1,2-dichloro-3-nitrobenzene, 4-ethylnitrobenzene, 2-vinylpyridine, 3-amino-1*H*-1,2,4-triazole, *N*-ethyl-*N*-nitrosourea, 5-aza-2′-deoxycytidine, ethynyl estradiol, 3-methylcholanthrene, phenobarbital, acetaminophen, isoniazid, capsaicin, *N*-deacetyl-*N*-methylcolchicine (Colcemid), 2.4-dinitrochlorobenzene, and dexamethasone were from Sigma Chemicals (St. Louis, MO). Methoprene acid, methoprene, all-*trans* retinoic acid, and 9-cis retinoic acid were from BIOMOL International L.P. (Plymouth Meeting, PA). Levothyroxine was from MP Biomedicals (Irvine, CA). 3-Iodo-2-propynyl butylcarbamate was from Olin Japan Inc. (Tokyo, Japan), *p*-chlorophenyl-3-iodopropargylformal was from Nagase ChemteX (Osaka, Japan), and 2,3,3,3–2′,3′,3′,3′-octachlorodipropylether was from Sankyo Chemical Industries, Ltd. (Tokyo, Japan). 1,2-Benzisothiazolin-3-one was from Riverson (Osaka, Japan), zinc butylxanthate was from Ouchishinko Chemical Industrial Co., Ltd. (Tokyo, Japan), and 4-amino-2,6-dichlorophenol was from Tokyo Kasei Kogyo Co. Ltd. (Tokyo, Japan).

**Hierarchical Clustering.** Hierarchical clustering analysis was carried out using the average linkage method and the "GeneSpring" software (Silicon Genetics, Inc., Redwood, CA). Pearson correlation coefficients were used to determine the degree of similarity.

## Results

**Sensitivity of JFCR39 to Chemicals.** Sensitivity of the JFCR39 panel of cells to 130 chemicals was determined as described under *Materials and Methods*. Table 1 summarizes

TABLE 2
$Log_{10}$ GI50 values of chemicals for each cell line in the JFCR-39 panel
Hi-conc means the highest concentration of the test chemical used. When the growth inhibition was over 50% at the Hi-Conc, $GI_{50}$ was assigned the Hi-Conc value.

| Exp-ID | S3416 | S3415 | S3413 | S3245 | S3117 | S3414 | S3118 | S3246 | S3125 | S3124 | S3123 | S1636 | S1635 | S1634 | S1718 |
|---|---|---|---|---|---|---|---|---|---|---|---|---|---|---|---|
| JCI No | −687 | −686 | −559 | −559 | −559 | −560 | −560 | −560 | −567 | −566 | −565 | −296 | −295 | −294 | −294 |
| Name or Abbr. | TTNPB | 13-*cis* | 9-*cis* | | | ATRA | | | SV-TF | SV-CA | SV-AHB | SV-NNK | SV-NN | DTBHQ | |
| Hi-Conc. | −4 | −4 | −4 | −4 | −4 | −4 | −4 | −4 | −4 | −4 | −4 | −4 | −4 | −4 | −4 |
| HBC-4 | −4.76 | −4.00 | −4.53 | −4.40 | −4.43 | −4.42 | −4.41 | −4.41 | −5.87 | −5.80 | −5.66 | −7.25 | −7.31 | −4.72 | −4.80 |
| BSY-1 | −4.78 | −4.16 | −4.60 | −4.73 | −4.73 | −4.69 | −4.70 | −4.81 | −6.31 | −6.06 | −5.76 | −6.93 | −7.34 | −5.07 | −4.93 |
| HBC-5 | −4.80 | −4.41 | −4.56 | −4.57 | −4.61 | −4.61 | −4.47 | −4.51 | −6.98 | −6.45 | −5.73 | −7.64 | −7.72 | −4.89 | −4.78 |
| MCF-7 | −4.73 | −4.35 | −4.40 | −4.39 | −4.48 | −4.48 | −4.54 | −4.66 | −5.87 | −5.78 | −5.68 | −6.77 | −7.08 | −5.29 | −5.25 |
| MDA-MB-231 | −4.75 | −4.21 | −4.70 | −4.55 | −4.69 | −4.63 | −4.53 | −4.65 | −5.90 | −5.86 | −5.84 | −6.84 | −7.39 | −5.52 | −5.30 |
| U251 | −4.77 | −4.14 | −4.61 | −4.51 | −4.61 | −4.57 | −4.45 | −4.63 | −6.45 | −5.76 | −5.70 | −6.85 | −7.44 | −4.96 | −5.11 |
| SF-268 | −4.75 | −4.00 | −4.24 | −4.55 | −4.40 | −4.47 | −4.48 | −4.76 | −5.90 | −5.79 | −5.70 | −7.53 | −7.67 | −4.77 | −4.81 |
| SF-295 | −4.80 | −4.29 | −4.54 | −4.66 | −4.60 | −4.59 | −4.48 | −4.57 | −6.19 | −5.80 | −5.74 | −6.89 | −6.97 | −4.87 | −4.97 |
| SF-539 | −4.95 | −4.35 | −4.75 | −4.80 | −4.79 | −4.80 | −4.71 | −4.76 | −6.39 | −5.96 | −5.81 | −7.79 | −7.75 | −4.79 | −4.86 |
| SNB-75 | −5.31 | −5.28 | −5.13 | −5.19 | | −4.71 | −4.69 | −4.87 | −6.41 | −6.33 | −5.93 | −7.60 | −7.70 | −4.67 | −4.80 |
| SNB-78 | −4.77 | −4.25 | −4.69 | −4.78 | −4.86 | −4.49 | −4.70 | −4.68 | −6.19 | −6.00 | −5.95 | −6.97 | −7.53 | −4.75 | −4.75 |
| HCC2998 | −4.68 | −4.00 | −4.48 | −4.61 | −4.62 | −4.55 | −4.62 | −4.76 | −5.91 | −5.75 | −5.67 | −6.47 | −6.77 | −4.82 | −4.75 |
| KM-12 | −4.70 | −4.00 | −4.46 | −4.51 | −4.48 | −4.51 | −4.47 | −4.58 | −5.93 | −5.80 | −5.65 | −6.77 | −6.87 | −4.74 | −4.77 |
| HT-29 | −4.73 | −4.00 | −4.47 | −4.53 | −4.50 | −4.60 | −4.52 | −4.56 | −5.90 | −5.80 | −5.56 | −5.89 | −6.78 | −4.80 | −4.89 |
| HCT-15 | −4.72 | −4.25 | −4.45 | −4.49 | −4.48 | −4.52 | −4.57 | −4.53 | −5.88 | −5.76 | −5.57 | −6.73 | −6.82 | −4.72 | −4.77 |
| HCT-116 | −4.77 | −4.07 | −4.67 | −4.59 | −4.67 | −4.71 | −4.61 | −4.64 | −6.46 | −6.10 | −5.77 | −6.58 | −6.82 | −4.98 | −5.13 |
| NCI-H23 | −4.74 | −4.00 | −4.47 | −4.60 | −4.59 | −4.61 | −4.55 | −4.63 | −6.11 | −5.75 | −5.72 | −6.86 | −7.42 | −4.76 | −4.90 |
| NCI-H226 | −4.72 | −4.00 | −4.61 | −4.68 | −4.78 | −4.80 | −4.54 | −5.48 | −5.95 | −5.81 | −5.76 | −6.73 | −6.78 | −4.89 | −4.91 |
| NCI-H522 | −4.72 | −4.45 | −4.68 | −4.82 | −4.77 | −4.71 | −4.71 | −4.68 | −6.45 | −5.99 | −5.78 | −7.62 | −7.46 | −5.37 | −5.37 |
| NCI-H460 | −4.70 | −4.00 | −4.55 | −4.63 | −4.58 | −4.68 | −4.55 | −4.49 | −5.96 | −5.82 | −5.72 | −7.44 | −7.42 | −4.84 | −4.84 |
| A549 | −4.79 | −4.00 | −4.72 | −4.77 | −4.78 | −4.70 | −4.62 | −4.53 | −5.91 | −5.79 | −5.71 | −6.80 | −6.83 | −4.83 | −4.87 |
| DMS273 | −4.57 | −4.21 | −4.50 | −4.62 | −4.55 | −4.57 | −4.51 | −4.49 | −6.20 | −5.81 | −5.72 | −7.43 | −7.44 | −4.91 | −4.98 |
| DMS114 | −4.77 | −4.16 | −4.33 | −4.62 | −4.49 | −4.51 | −4.53 | −4.61 | −6.66 | −6.33 | −5.77 | −6.83 | −6.88 | −5.12 | −5.21 |
| LOX-IMVI | −4.77 | −4.69 | −4.68 | −4.66 | −4.70 | −4.77 | −4.74 | −4.74 | −6.75 | −6.59 | −5.76 | −6.86 | −6.94 | −5.05 | −5.15 |
| OVCAR-3 | −4.77 | −4.38 | −4.56 | −4.67 | −4.72 | −4.64 | −4.62 | −4.71 | −6.61 | −6.13 | −5.89 | −6.77 | −6.79 | −4.89 | −4.86 |
| OVCAR-4 | −4.72 | −4.05 | −4.63 | −4.64 | −4.64 | −4.58 | −4.39 | −4.54 | −6.73 | −6.23 | −5.80 | −6.82 | −6.90 | −5.13 | −4.90 |
| OVCAR-5 | −4.75 | −4.00 | −4.33 | −4.39 | −4.42 | −4.44 | −4.34 | −4.44 | −5.92 | −5.74 | −5.67 | −6.46 | −6.71 | −5.22 | −5.26 |
| OVCAR-8 | −4.75 | −4.23 | −4.50 | −4.53 | −4.59 | −4.66 | −4.67 | −4.70 | −5.95 | −5.77 | −5.69 | −6.82 | −6.84 | −4.64 | −4.70 |
| SK-OV-3 | −4.79 | −4.00 | −4.49 | −4.51 | −4.81 | −4.52 | −4.54 | −4.50 | −5.76 | −5.64 | −4.91 | −6.75 | −6.76 | −4.64 | −4.74 |
| RXF-631L | −4.77 | −4.00 | −4.54 | −4.58 | −4.60 | −4.72 | −4.63 | −4.61 | −5.91 | −5.80 | −5.59 | −7.13 | −7.46 | −4.81 | −4.84 |
| ACHN | −4.73 | −4.00 | −4.56 | −4.66 | −4.56 | −4.50 | −4.40 | −4.76 | −5.90 | −5.79 | −5.73 | −6.74 | −6.80 | −4.71 | −4.83 |
| St-4 | −4.74 | −4.00 | −4.42 | −4.54 | −4.65 | −4.53 | −4.49 | −4.57 | −5.91 | −5.81 | −5.76 | −7.65 | −7.70 | −4.68 | −4.75 |
| MKN1 | −4.75 | −4.33 | −4.56 | −4.63 | −4.62 | −4.56 | −4.45 | −4.48 | −6.15 | −5.81 | −5.78 | −7.67 | −7.68 | −4.59 | −4.81 |
| MKN7 | −4.78 | −4.40 | −4.68 | −4.59 | −4.70 | −4.73 | −4.56 | −4.65 | −6.29 | −5.85 | −5.76 | −6.70 | −6.90 | −4.79 | −4.84 |
| MKN28 | −4.71 | −4.28 | −4.56 | −4.59 | −4.59 | −4.65 | −4.56 | −4.60 | −6.10 | −5.93 | −5.68 | −6.51 | −6.81 | −4.72 | −4.89 |
| MKN45 | −4.72 | −4.00 | −4.51 | −4.41 | −4.46 | −4.73 | −4.41 | −4.43 | −6.06 | −5.90 | −5.69 | −6.71 | −6.82 | −4.71 | −4.87 |
| MKN74 | −4.74 | −4.40 | −4.61 | −4.63 | −4.61 | −4.73 | −4.68 | −4.67 | −5.97 | −5.92 | −5.61 | −6.92 | −7.00 | −5.10 | −5.42 |
| DU-145 | −4.68 | −4.00 | −4.25 | −4.78 | −4.41 | −4.42 | −4.44 | −4.54 | −6.08 | −5.82 | −5.75 | −7.43 | −7.55 | −4.59 | −5.02 |
| PC-3 | −4.74 | −4.00 | −4.58 | −4.65 | −4.48 | −4.74 | −4.39 | −4.51 | −5.83 | −5.77 | −5.61 | −6.67 | −6.69 | −4.89 | −4.74 |

abbreviations, applications, targets, and known mechanisms of 130 chemicals and 21 anticancer drugs. Approximately 15% of the chemicals were assessed twice or more. Approximately 40% of the chemicals tested had little effect on the growth of cells in the JFCR39 panel. However, the rest of the chemicals significantly inhibited the cell growth across the JFCR39 panel. For example, Fig. 1 shows the dose response curves of the cells in the JFCR39 panel against digoxin. The concentration at which the cell growth is inhibited by 50% represents GI50. Figure 2 shows the fingerprints of four chemicals [digoxin, ouabain, snake venom from *N. nigricollis* (SV-NN), and snake venom from *N. naja kaouthia* (SV-NNK)], which differentially inhibited the growth of cells in the JFCR39 panel; these fingerprints were drawn based on a calculation using a set of GI50s and clearly represented the GI50 pattern. These results were highly reproducible in that the Pearson correlation coefficient of the duplicate experiments for digoxin was 0.839 ($p < 0.001$) and that for ouabain was 0.864 ($p < 0.001$). It is noteworthy that, digoxin and ouabain, both of which are cardiac glycosides and inhibit Na-K ATPase, showed similar fingerprints. The fingerprints of SV-NNK and SV-NN, which belong to the elapidae, known as cobras, were also similar, but were different from the fingerprints of digoxin and ouabain. Table 2 summarizes only a portion of the GI50 values from 160 experiments involving 130 chemicals and 42 experiments involving 21 anticancer drugs. GI50 values from all experiments are described in the Supplemental Data (Table S1). All these data were stored in a chemosensitivity database and used for further analysis.

**Classification of the Chemicals by Hierarchical Clustering.** Sixty-nine chemicals were selected for further analysis based on the following criteria: 1) GI50 values for the test chemical can be determined for at least 10 cell lines in the JFCR39 panel, and 2) the range of log GI50 for the test chemical is more than 0.6, suggesting differential growth inhibition. We analyzed the GI50 values of these 69 chemicals and 20 anticancer drugs by hierarchical clustering analysis (Fig. 3). We found approximately 12 clusters (threshold: $r = 0$, Fig. 3, clusters A–L), which were further divided into 49 subclusters (threshold: $r = 0.408$, Fig. 3, clusters A1–L6).

**Analysis of Clusters.** Most anticancer drugs we have tested belonged either to cluster A or cluster H, depending on their modes of action (Dan et al., 2002). The targets of the anticancer drugs belonging to the cluster A were related to DNA (Topo I, antimetabolite of pyridine, DNA alkylator) and the target of the anticancer drugs belonging to the cluster H was tubulin. We presently found that cisplatin exceptionally belonged to cluster F2, not cluster A, although it is known to cross-link DNA strands (Jamieson and Lippard, 1999; Wong and Giandomenico, 1999). We were also able to precisely group the clusters into several subclusters having similar characteristics. For example, the cardiac glycosides digoxin and ouabain were grouped in one cluster (cluster F3). SV-

| S3243 | S3244 | S1534 | S3237 | S3238 | S1525 | S3236 | S1928 | S1421 | S1705 | S1327 | S1413 | S1413 | S3408 | S3409 | S2421 |
|---|---|---|---|---|---|---|---|---|---|---|---|---|---|---|---|
| −599 | −599 | −270 | −270 | −270 | −261 | −261 | −261 | −247 | −247 | −232 | −232 | −232 | −421 | −421 | −421 |
| Thiram | | Ziram | | | Paraquat | | | Ouabain | | Digoxin | | | TBT | | |
| −4 | −4 | −4 | −4 | −4 | −4 | −3 | −4 | −4 | −6 | −4 | −4 | −4 | −4 | −4 | −4 |
| −4.71 | −4.79 | −5.80 | −5.73 | −5.70 | −4.00 | −3.61 | −4.00 | −7.54 | −7.28 | −6.57 | −6.96 | −6.96 | −6.79 | −6.77 | −6.72 |
| −6.97 | −7.12 | −6.85 | −6.76 | −6.60 | −4.00 | −4.45 | −4.51 | −8.00 | −7.76 | −7.58 | −7.68 | −7.68 | −7.03 | −7.01 | −6.83 |
| −7.41 | −7.66 | −7.18 | −7.47 | −7.47 | −4.68 | −4.70 | | −7.76 | −7.51 | −7.15 | −7.44 | −7.44 | −6.76 | −6.88 | −6.83 |
| −4.77 | −4.80 | −6.00 | −5.84 | −5.83 | −4.06 | −3.72 | −4.00 | −7.64 | −7.51 | −7.29 | −7.39 | −7.39 | −6.86 | −6.84 | −6.79 |
| −4.66 | −4.68 | −5.64 | −5.75 | −5.63 | −4.00 | −3.57 | −4.00 | −7.40 | −6.81 | −6.41 | −6.72 | −6.72 | −6.83 | −6.81 | −6.70 |
| −4.75 | −4.78 | −5.71 | −5.79 | −5.82 | −4.00 | −3.69 | −4.00 | −7.75 | −7.16 | −7.01 | −7.40 | −7.40 | −6.79 | −6.77 | −6.72 |
| −4.86 | −4.96 | −5.74 | −5.83 | −7.01 | −4.00 | −4.08 | −4.00 | −8.00 | −7.77 | −7.42 | −7.70 | −7.70 | −6.84 | −6.85 | −6.71 |
| −4.77 | −4.89 | −5.71 | −5.70 | −5.79 | −4.47 | −4.37 | −4.20 | −8.00 | −7.64 | −7.42 | −7.55 | −7.55 | −6.75 | −6.73 | −6.76 |
| −4.75 | −4.88 | −5.73 | −5.75 | −5.77 | −4.00 | −4.03 | −4.00 | −8.00 | −7.70 | −7.46 | −7.63 | −7.63 | −6.77 | −6.72 | −6.67 |
| −4.71 | −4.96 | −5.79 | −5.92 | −5.80 | −4.00 | −3.94 | −4.00 | −7.70 | −7.45 | −6.86 | −7.40 | −7.40 | −6.99 | −6.95 | −7.05 |
| −4.70 | −4.78 | −5.69 | −5.64 | −5.69 | −4.00 | −3.78 | −4.00 | −7.98 | −7.64 | −7.45 | −7.60 | −7.60 | −6.72 | −6.79 | −6.70 |
| −4.82 | −4.69 | −5.76 | −5.79 | −5.81 | −4.00 | −3.70 | −4.00 | −7.64 | −6.77 | −6.68 | −7.25 | −7.25 | −6.77 | −6.79 | −6.72 |
| −4.80 | −4.80 | −5.43 | −5.74 | −5.73 | −4.00 | −3.58 | −4.00 | −7.67 | −7.12 | −6.69 | −7.34 | −7.34 | −7.00 | −6.98 | −6.74 |
| −4.68 | −4.85 | −5.75 | −5.77 | −5.76 | −4.10 | −4.03 | −4.07 | −7.75 | −7.31 | −7.20 | −7.34 | −7.34 | −6.89 | −6.84 | −6.66 |
| −4.68 | −4.75 | −5.70 | −5.72 | −5.83 | −4.00 | −3.64 | −4.00 | −7.74 | −7.63 | −6.92 | −7.54 | −7.54 | −6.88 | −6.84 | −6.70 |
| −4.72 | −4.72 | −5.74 | −5.68 | −5.77 | −4.00 | −3.60 | −4.00 | −8.00 | −7.57 | −7.47 | −7.62 | −7.62 | −6.90 | −6.85 | −6.74 |
| −4.69 | −4.78 | −5.96 | −5.85 | −5.84 | −4.19 | −4.18 | −4.00 | −8.00 | −7.67 | −7.50 | −7.84 | −7.84 | −6.90 | −6.85 | −6.76 |
| −6.33 | −6.74 | −5.63 | −5.96 | −6.12 | −4.41 | −4.41 | −4.00 | −8.00 | −7.37 | −6.93 | −7.61 | −7.61 | −6.99 | −6.91 | −6.74 |
| −7.49 | −7.50 | −7.44 | −7.66 | −8.00 | −4.49 | −4.71 | −4.59 | −8.00 | −7.64 | −7.59 | −7.91 | −7.91 | −6.83 | −6.80 | −6.25 |
| −6.14 | −6.16 | −6.30 | −6.10 | −6.15 | −4.30 | −4.45 | −4.37 | −8.00 | −7.74 | −7.60 | −7.77 | −7.77 | −6.98 | −6.98 | −6.56 |
| −4.84 | −4.82 | −5.97 | −5.91 | −5.91 | −4.49 | −4.49 | −4.41 | −8.00 | −7.80 | −7.66 | −7.91 | −7.91 | −6.82 | −6.87 | −6.73 |
| −6.64 | −6.58 | −6.43 | −6.84 | −6.82 | −4.25 | −4.43 | −4.30 | −8.00 | −7.71 | −7.48 | −7.72 | −7.72 | −6.74 | −6.75 | −6.70 |
| −7.18 | −7.39 | −7.37 | −7.38 | −7.43 | −4.50 | −4.63 | −4.27 | −8.00 | −7.84 | −7.73 | −8.00 | −8.00 | −7.11 | −7.12 | −7.02 |
| −4.68 | −4.71 | −5.66 | −5.71 | −5.70 | −4.00 | −3.51 | −4.00 | −7.80 | −7.80 | −7.39 | −7.46 | −7.46 | −6.93 | −6.94 | −6.76 |
| −4.86 | −6.25 | −6.07 | −6.35 | −6.32 | −4.00 | −4.46 | −4.28 | −8.00 | −7.66 | −7.64 | −7.59 | −7.59 | −6.80 | −6.82 | −6.74 |
| −4.77 | −6.67 | −5.90 | −5.91 | −5.87 | −4.00 | −4.21 | −4.48 | −8.00 | −7.71 | −7.71 | −7.72 | −7.72 | −6.91 | −7.20 | −6.80 |
| −4.90 | −6.00 | −6.11 | −6.91 | −6.74 | −4.00 | −3.98 | −4.00 | −7.89 | −7.62 | −7.12 | −7.42 | −7.42 | −6.90 | −6.93 | −6.75 |
| −4.62 | −4.74 | −5.59 | −5.68 | −5.67 | −4.00 | −3.84 | −4.00 | −7.85 | −7.44 | −6.97 | −7.29 | −7.29 | −6.73 | −6.67 | −6.57 |
| −4.39 | −4.38 | −4.92 | −5.49 | −5.53 | −4.00 | −3.39 | −4.00 | −7.74 | −7.67 | −7.18 | −7.38 | −7.38 | −6.80 | −6.77 | −6.68 |
| −4.75 | −4.65 | −5.57 | −5.63 | −5.60 | −4.00 | −3.60 | −4.00 | −7.10 | −6.00 | −6.42 | −6.20 | −6.20 | −6.78 | −6.76 | −6.68 |
| −4.52 | −4.60 | −5.64 | −5.68 | −5.69 | −4.00 | −3.51 | −4.00 | −8.00 | −7.72 | −7.44 | −7.59 | −7.59 | −6.78 | −6.77 | −6.76 |
| −4.59 | −4.72 | −5.99 | −5.73 | −5.81 | −4.00 | −3.58 | −4.00 | −8.00 | −7.65 | −7.45 | −7.60 | −7.60 | −6.80 | −6.80 | −6.72 |
| −4.80 | −4.85 | −6.82 | −5.84 | −5.92 | −4.41 | −4.61 | −4.48 | −8.00 | −7.72 | −7.68 | −7.72 | −7.72 | −7.25 | −7.15 | −6.87 |
| −4.79 | −4.82 | −6.56 | −5.84 | −5.82 | −4.08 | −4.29 | −4.32 | −7.80 | −7.48 | −6.98 | −7.47 | −7.47 | −7.34 | −7.07 | −6.86 |
| −7.18 | −7.21 | −5.82 | −7.09 | −7.13 | −4.00 | −4.40 | −4.18 | −7.70 | −7.42 | −6.77 | −7.37 | −7.37 | −6.84 | −6.82 | −6.87 |
| −6.65 | −6.71 | −6.05 | −7.18 | −6.86 | −4.00 | −4.29 | −4.35 | −7.77 | −7.25 | −6.99 | −7.52 | −7.52 | −6.96 | −6.97 | −6.87 |
| −7.05 | −7.08 | −6.35 | −5.86 | −7.05 | −4.00 | −4.47 | −4.06 | −7.91 | −7.65 | −7.55 | −7.74 | −7.74 | −6.97 | −7.37 | −7.05 |
| −4.47 | −4.70 | −5.68 | −5.68 | −5.65 | −4.00 | −3.57 | −4.00 | −8.00 | −7.64 | −7.59 | −7.71 | −7.71 | −6.90 | −6.89 | −6.70 |
| −4.42 | −4.77 | −5.61 | −5.53 | −5.56 | −4.00 | −3.64 | −4.37 | −8.00 | −7.62 | −7.41 | −7.62 | −7.62 | −6.77 | −6.78 | −6.73 |

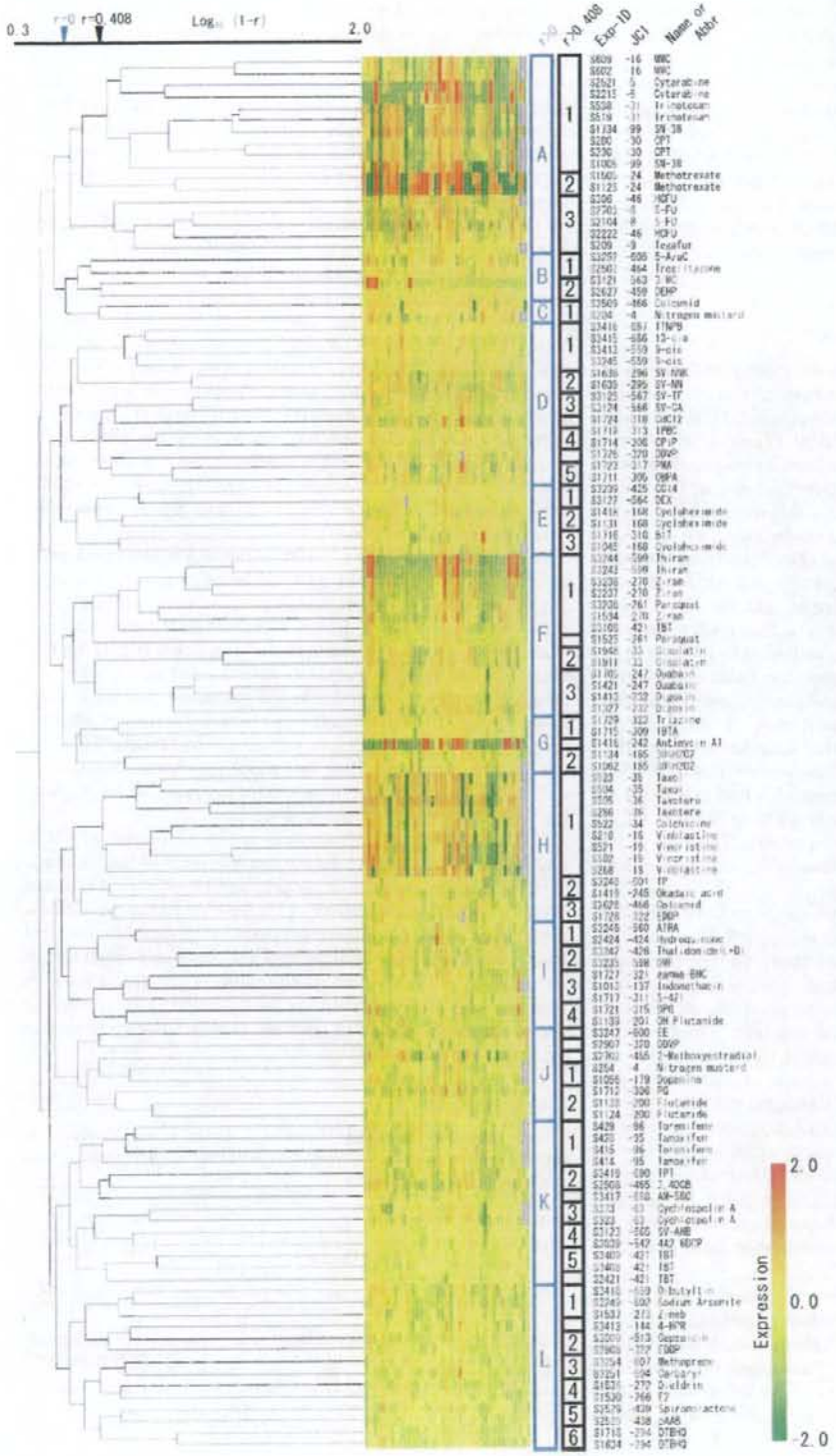


**Fig. 3.** Hierarchical clustering of 69 test chemicals and 20 anticancer drugs based on their GI50 values. Hierarchical clustering method was an "average linkage method" using the Pearson correlation as distance. We classified the chemicals into two kinds of clusters; their threshold values were $r = 0$ and $r = 0.408$ ($p < 0.01$), respectively. Gradient color indicates relative level (log transformed) of GI50. Red, more sensitive than the mean GI50 (2.0); yellow, mean GI50 (0.0); and green, less sensitive than the mean GI50 (−2.0). On the color scale, red represents the GI50 value that is 100-fold higher than the mean GI50.

NNK and SV-NN, on the other hand, belonged to the cluster D2. These results are in accordance with the similar fingerprints shown in Fig. 2. It is noteworthy that the snake venoms from the *C. atrox* and *T. flavoviridis*, species belonging to the viperidae family of snakes, formed another cluster (cluster D3), which was different from that of the elapidae family of snakes, *N. naja kaouthia* and *N. nigricollis*. 9-*cis* Retinoic acid, 13-*cis* retinoic acid, and 4-[*E*-2-(5,6,7,8-tetrahydro-5,5,8,8-tetra-methyl-2-naphthalenyl)-1-propenyl]benzoic acid, which are RAR agonists (Aström et al., 1990), also formed a separate cluster (cluster D1). Likewise, agricultural chemicals paraquat, ziram, and thiram formed a single cluster (cluster F1).

## Discussion

The JFCR39 system coupled to a drug activity database is a good model for investigating the diversity of chemosensitivity in cancer cells. We have previously established panels of human cancer cell lines [JFCR39 (Yamori, 2003) and JFCR45 (Nakatsu et al., 2005)]. We used these panels of cells to demonstrate that they provide powerful means to predict the action mechanisms of drugs, and also used them to identify new target compounds. In this manuscript, we used the JFCR39 system to evaluate various chemicals (such as toxic chemicals, agricultural chemicals, and synthetic intermediates), which are not anticancer drugs, and classified them according to their molecular target or action mechanism. As a result, these chemicals were classified into a number of clusters. Our results also suggested that each cluster consisted of chemicals sharing a common action mechanism.

We determined the growth inhibition of cells in the JFCR39 panel by 130 chemicals and calculated their GI50 values. Some of the chemicals were assessed twice or more to confirm the reproducibility of the assay. We had to exclude 61 chemicals from further analysis because they did not inhibit the cells in the JFCR39 panel significantly. The rest of the chemicals (69 of 130, ~60%) met our selection criteria and were evaluated by cluster analysis.

First, we found that the chemicals tested in duplicate formed tight clusters, showing high reproducibility. Next, we investigated the difference between these 69 test chemicals and the anticancer drugs. Sixty-nine chemicals, which are not anticancer drugs, formed several clusters, which were different from the anticancer drug clusters. These results suggest that the action mechanisms of these chemicals are different from the action mechanisms of the anticancer drugs. However, we found that cisplatin did not belong to the cluster A, which consisted of DNA-targeting anticancer drugs. We do not understand the reason at present. However, there is a possibility that cisplatin has other action mechanisms, which may have made the fingerprint of cisplatin different from those of other DNA-targeting drugs. Indeed, cisplatin is known to form DNA-protein cross-links (Zwelling et al., 1979; Chválová et al., 2007).

Our analysis also identified several interesting clusters. For example, the cluster F3 consisted of cardiac glycosides digoxin and ouabain, both of which inhibit Na-K ATPase (Reuter et al., 2002). The cluster D1 consisted of 9-*cis* retinoic acid, 13-*cis* retinoic acid, and 4-[*E*-2-(5,6,7,8-tetrahydro-5,5,8,8-tetra-methyl-2-naphthalenyl)-1-propenyl]benzoic acid, which are RAR agonists. These results suggest that chemicals other than the anticancer drugs also form clusters when they share the same action mechanisms. It is noteworthy that SV-NNK and SV-NN, from snakes that belonged to the elapidae family, formed one cluster (cluster D2). In contrast, the snake venoms from the *C. atrox* and *T. flavoviridis*, which belonged to the viperidae family, formed a cluster (cluster D3) different from the elapidae cluster. These results are reasonable because snake venoms from different snake families are known to differ not only in composition but also in levels of toxicity and mechanisms of action.

The agricultural chemicals paraquat, ziram, and thiram were also classified into a single cluster (cluster F1). Among these agricultural chemicals, the action mechanism of ziram is not known. However, both paraquat and thiram are known to induce oxidative stress (Cereser et al., 2001; Suntres, 2002). Therefore, based on our observations, we could suggest that ziram also acted by inducing oxidative stress. The agricultural chemicals methoprene (insect growth regulator) and carbaryl (chorine esterase inhibitor) formed cluster L3, although their common mechanism is unknown. Cluster D4 and D5 consist of the antibacterial agents or fungicides. 3-Iodo-2-propynyl-butylcarbamate and *p*-chlorophenyl-3′-iodopropargylformal, belonging to cluster D4, are the iodo-type antibacterial agents.

Thus, cluster analysis of GI50 values of various chemicals, determined using the JFCR39 cell panel, suggests that the JFCR39 system could, at least in part, allow classification of chemical compounds on the basis of their action mechanisms. Our analysis also suggests that the chemicals belonging the same cluster share a common action mechanism. We are going to develop a larger library of reference chemicals with known action mechanisms (i.e., various inhibitors of biological pathways), and expand our database by integrating their GI50 measurements, which will make the cluster analysis as well as the COMPARE analysis more informative for predicting the mechanism of test chemicals.

In conclusion, to evaluate the potential of the JFCR39 system in predicting the action mechanisms of toxic chemicals, we investigated the fingerprints of 130 different types of chemical compounds including toxic chemicals, pesticides, drugs, and synthetic intermediates. Using the hierarchical clustering analysis, we classified 69 chemicals, at least in part, based on their action mechanisms. Thus, this approach using the JFCR39 cell panel is useful not only in predicting the action mechanisms of toxic chemicals but also in evaluating their toxicity.

#### Acknowledgments

We thank Yumiko Mukai, Yumiko Nishimura, and Mariko Seki for determination of chemosensitivity and Satoshi Kitajima for help with chemical information.

#### References

Akashi T, Nishimura Y, Wakatabe R, Shiwa M, and Yamori T (2007) Proteomics-based identification of biomarkers for predicting sensitivity to a PI3-kinase inhibitor in cancer. *Biochem Biophys Res Commun* **352**:514–521.

Akashi T and Yamori T (2007) A novel method for analyzing phosphoproteins using SELDI-TOF MS in combination with a series of recombinant proteins. *Proteomics* **7**:2350–2354

Aström A, Pettersson U, Krust A, Chambon P, and Voorhees JJ (1990) Retinoic acid and synthetic analogs differentially activate retinoic acid receptor dependent transcription. *Biochem Biophys Res Commun* **173**:339–345.

Cereser C, Boget S, Parvaz P, and Revol A (2001) An evaluation of thiram toxicity on cultured human skin fibroblasts. *Toxicology* **162**:89–101.

Chválová K, Brabec V, and Kasparkova J (2007) Mechanism of the formation of DNA-protein cross-links by antitumor cisplatin. *Nucleic Acids Res* **35**:1812–1821.

Dan S, Shirakawa M, Mukai Y, Yoshida Y, Yamazaki K, Kawaguchi T, Matsuura M, Nakamura Y, and Yamori T (2003) Identification of candidate predictive markers of anticancer drug sensitivity using a panel of human cancer cell lines. *Cancer Sci* **94:**1074–1082.

Dan S, Tsunoda T, Kitahara O, Yanagawa R, Zembutsu H, Katagiri T, Yamazaki K, Nakamura Y, and Yamori T (2002) An integrated database of chemosensitivity to 55 anticancer drugs and gene expression profiles of 39 human cancer cell lines. *Cancer Res* **62:**1139–1147.

Hershberger LG, Shipley EG, and Meyer RK (1953) Myotrophic activity of 19-nortestosterone and other steroids determined by modified levator ani muscle method. *Proc Soc Exp Biol Med* **83:**175–180.

Jamieson ER and Lippard SJ (1999) Structure, Recognition, and Processing of Cisplatin-DNA Adducts. *Chem Rev* **99:**2467–2498.

Kanno J, Kato H, Iwata T, and Inoue T (2002) Phytoestrogen-low diet for endocrine disruptor studies. *J Agric Food Chem* **50:**3883–3885.

Naasani I, Seimiya H, Yamori T, and Tsuruo T (1999) FJ5002: a potent telomerase inhibitor identified by exploiting the disease-oriented screening program with COMPARE analysis. *Cancer Res* **59:**4004–4011.

Nakamura H, Dan S, Akashi T, Unno M, and Yamori T (2007) Absolute quantification of four isoforms of the class I phosphoinositide-3-kinase catalytic subunit by real-time RT-PCR. *Biol Pharm Bull* **30:**1181–1184.

Nakatsu N, Yoshida Y, Yamazaki K, Nakamura T, Dan S, Fukui Y, and Yamori T (2005) Chemosensitivity profile of cancer cell lines and identification of genes determining chemosensitivity by an integrated bioinformatical approach using cDNA arrays. *Mol Cancer Ther* **4:**399–412.

Okutsu J, Tsunoda T, Kaneta Y, Katagiri T, Kitahara O, Zembutsu H, Yanagawa R, Miyawaki S, Kuriyama K, Kubota N, et al. (2002) Prediction of chemosensitivity for patients with acute myeloid leukemia, according to expression levels of 28 genes selected by genome-wide complementary DNA microarray analysis. *Mol Cancer Ther* **1:**1035–1042.

Paull KD, Shoemaker RH, Hodes L, Monks A, Scudiero DA, Rubinstein L, Plowman J, and Boyd MR (1989) Display and analysis of patterns of differential activity of drugs against human tumor cell lines: development of mean graph and COMPARE algorithm. *J Natl Cancer Inst* **81:**1088–1092.

Reuter H, Henderson SA, Han T, Ross RS, Goldhaber JI, and Philipson KD (2002) The $Na^+$–$Ca^{2+}$ exchanger is essential for the action of cardiac glycosides. *Circ Res* **90:**305–308.

Scherf U, Ross DT, Waltham M, Smith LH, Lee JK, Tanabe L, Kohn KW, Reinhold WC, Myers TG, Andrews DT, et al. (2000) A gene expression database for the molecular pharmacology of cancer. *Nat Genet* **24:**236–244.

Suntres ZE (2002) Role of antioxidants in paraquat toxicity. *Toxicology* **180:**65–77.

Weinstein JN, Kohn KW, Grever MR, Viswanadhan VN, Rubinstein LV, Monks AP, Scudiero DA, Welch L, Koutsoukos AD, and Chiausa AJ (1992) Neural computing in cancer drug development: predicting mechanism of action. *Science* **258:**447–451.

Weinstein JN, Myers TG, O'Connor PM, Friend SH, Fornace AJ Jr, Kohn KW, Fojo T, Bates SE, Rubinstein LV, Anderson NL, et al. (1997) An information-intensive approach to the molecular pharmacology of cancer. *Science* **275:**343–349.

Wong E and Giandomenico CM (1999) Current status of platinum-based antitumor drugs. *Chem Rev* **99:**2451–2466.

Yaguchi S, Fukui Y, Koshimizu I, Matsuno T, Gouda H, Hirono S, Yamazaki K, and Yamori T (2006) Antitumor activity of ZSTK474, a new phosphatidyl inositol 3-kinase inhibitor. *J Natl Cancer Inst* **98:**545–556.

Yamori T (2003) Panel of human cancer cell lines provides valuable database for drug discovery and bioinformatics. *Cancer Chemother Pharmacol* **52 (Suppl 1):** S74–S79

Yamori T, Matsunaga A, Sato S, Yamazaki K, Komi A, Ishizu K, Mita I, Edatsugi H, Matsuba Y, Takezawa K, et al. (1999) Potent antitumor activity of MS-247, a novel DNA minor groove binder, evaluated by an in vitro and in vivo human cancer cell line panel. *Cancer Res* **59:**4042–4049.

Zembutsu H, Ohnishi Y, Tsunoda T, Furukawa Y, Katagiri T, Ueyama Y, Tamaoki N, Nomura T, Kitahara O, Yanagawa R, et al. (2002) Genome-wide cDNA microarray screening to correlate gene expression profiles with sensitivity of 85 human cancer xenografts to anticancer drugs. *Cancer Res* **62:**518–527.

Zwelling LA, Anderson T, and Kohn KW (1979) DNA-protein and DNA interstrand cross-linking by cis- and trans-platinum(II) diamminedichloride in L1210 mouse leukemia cells and relation to cytotoxicity. *Cancer Res* **39:**365–369.

**Address correspondence to:** Takao Yamori, Division of Molecular Pharmacology, Cancer Chemotherapy Center, Japanese Foundation for Cancer Research, 3-10-6, Ariake, Koto-ku, Tokyo 135-8550, Japan. E-mail: yamori@jfcr.or.jp, 07a$sl

ELSEVIER

Bone 40 (2007) 876–887

BONE

www.elsevier.com/locate/bone

# Effects of aromatase inhibitors on human osteoblast and osteoblast-like cells: A possible androgenic bone protective effects induced by exemestane

Yasuhiro Miki [a], Takashi Suzuki [a], Masahito Hatori [b], Katsuhide Igarashi [c], Ken-ich Aisaki [c], Jun Kanno [c], Yasuhiro Nakamura [a], Miwa Uzuki [d], Takashi Sawai [c], Hironobu Sasano [a,*]

[a] *Department of Pathology, Tohoku University Graduate School of Medicine, 2-1 Seiryo-machi, Aoba-ku, Sendai, Miyagi, 980-8575, Japan*
[b] *Department of Orthopedic Surgery, Tohoku University Graduate School of Medicine, Sendai, Japan*
[c] *Division of Toxicology, National Institute of Health Sciences, Biological Safety Research Center, Setagaya, Tokyo, Japan*
[d] *Department of Pathology, Iwate Medical College, Morioka, Japan*

Received 21 April 2006; revised 6 November 2006; accepted 14 November 2006
Available online 28 December 2006

**Abstract**

Effects of aromatase inhibitors (AIs) on the human skeletal system due to systemic estrogen depletion are becoming clinically important due to their increasing use as an adjuvant therapy in postmenopausal women with breast cancer. However, possible effects of AIs on human bone cells have remained largely unknown. We therefore studied effects of AIs including the steroidal AI, exemestane (EXE), and non-steroidal AIs, Aromatase Inhibitor I (AI-I) and aminoglutethimide (AGM), on a human osteoblast. We employed a human osteoblast cell line, hFOB, which maintains relatively physiological status of estrogen and androgen pathways of human osteoblasts, i.e., expression of aromatase, androgen receptor (AR), and estrogen receptor (ER) β. We also employed osteoblast-like cell lines, Saos-2 and MG-63 which expressed aromatase, AR, and ERα/β in order to further evaluate the mechanisms of effects of AIs on osteoblasts. There was a significant increment in the number of the cells following 72 h treatment with EXE in hFOB and Saos-2 but not in MG-63, in which the level of AR mRNA was lower than that in hFOB and Saos-2. Alkaline phosphatase activity was also increased by EXE treatment in hFOB and Saos-2. Pretreatment with the AR blocker, flutamide, partially inhibited the effect of EXE. AI-I exerted no effects on osteoblast cell proliferation and AGM diminished the number of the cells. hFOB converted androstenedione into E2 and testosterone (TST). Both EXE and AI-I decreased E2 level and increased TST level. In a microarray analysis, gene profile patterns following treatment with EXE demonstrated similar patterns as with DHT but not with E2 treatment. The genes induced by EXE treatment were related to cell proliferation, differentiation which includes genes encoding cytoskeleton proteins. We also examined the expression levels of these genes using quantitative RT-PCR in hFOB and Saos-2 treated with EXE and DHT and with/without flutamide. HOXD11 gene known as bone morphogenesis factor and osteoblast growth-related genes were induced by EXE treatment as well as DHT treatment in both hFOB and Saos-2. These results indicated that the steroidal aromatase inhibitor, EXE, stimulated hFOB cell proliferation via both AR dependent and independent pathways.


*Keywords:* Osteoblast; Aromatase inhibitor; Androgen; Estrogen; Exemestane

## Introduction

Results in various epidemiological or clinical studies demonstrated that estrogens play important protective roles in human skeletal as well as cardiovascular systems, and estrogen deficiency resulted in accelerating the development of osteoporosis in postmenopausal women [1–3]. In breast cancer of postmenopausal women, hormone therapies without any clinically deleterious effects due to estrogen deficiency on bone metabolism as well as lipid metabolisms are preferable. Estrogen deficiency has been generally detected in the patients with breast cancer following chemotherapy induced ovarian failure, gonadotropin analogue, and aromatase inhibitors (AIs) therapy [4]. Aromatase is the pivotal enzyme of *in situ* or intratumoral estrogen biosynthesis in postmenopausal breast cancer patients, and catalyzes the conversion from androgens into estrogens (Fig. 1A). AIs therefore play an important role in

* Corresponding author. Fax: +81 22 273 5976.
*E-mail address:* hsasano@patholo2.med.tohoku.ac.jp (H. Sasano).

8756-3282/$ - see front matter © 2006 Elsevier Inc. All rights reserved.
doi:10.1016/j.bone.2006.11.029

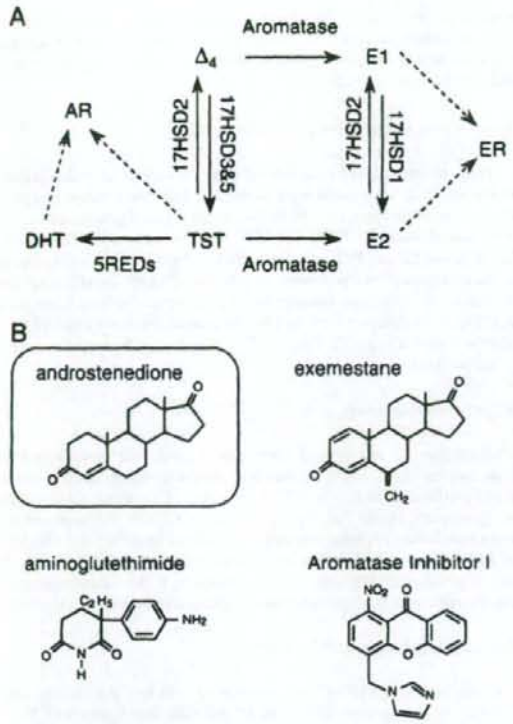


Fig. 1. (A) Summary of the pathway of estrogens and androgens production. Aromatase catalyzes the change from androstenedione (Δ4) and testosterone (TST) into estrone (E1) and estradiol (E2), respectively. 17HSD, 17β-hydroxysteroid dehydrogenase; 5REDs, 5α-reductase types 1 and 2; AR, androgen receptor; DHT, 5α-dihydrotestosterone; ER, estrogen receptor. (B) Structure of aromatase inhibitors used in this study. Androstenedione is a natural substrate of aromatase. Steroidal aromatase inhibitor, exemestane has an androstenedione-like structure.

clinical management of both primary and advanced breast cancer in postmenopausal women [5]. AIs are classified into two classes according to their modes of action. Type I AIs are steroidal inhibitions and one of them, exemestane (EXE) inhibits aromatase irreversibly and has an androstenedione ($\Delta_4$)-like structure (Fig. 1B) [5–7]. Type II AIs are non-steroidal inhibitions and include aminoglutethimide (AGM), anastrozole, and letrozole [5].

Results of *in vivo* study using ovariectomized (OVX) rats demonstrated that EXE and its principal metabolite form, 17-hydroexemestane (17H-EXE) but not letrozole significantly prevented bone loss in OVX rats [8,9]. EXE and its principal metabolite, 17H-EXE, are structurally related to $\Delta_4$ and bind to androgen receptor (AR) with relatively low affinity compared to 5α-dihydrotestosterone (DHT) [7]. These finding suggest that EXE may demonstrate protective effects toward bone tissues through its androgenic actions. However, detailed mechanisms of effects of EXE or androgen itself on human bone cells have remained largely unknown.

Various studies using human or animal bone tissues [10,11] and osteoblast cell culture using osteosarcoma cells [12,13] demonstrated that aromatase mRNA or protein was detected in osteoblast cells, which play an important role in bone remodeling. Therefore, in this study, we focused on effects of EXE in human osteoblast in an initial attempt to evaluate the effects of these AIs (summarized in Table 1 and Fig. 1B) [5–7,14], including AGM, EXE, and an experimental compound for inhibition of aromatase, Aromatase Inhibitor I (AI-I) [14] on human osteoblast and osteoblast-like cell lines. In our present study, we employed normal human cell line, hFOB, which maintains native characteristics of sex steroid hormone pathway of human osteoblasts, i.e., expression of AR, ERβ but not ERα, and aromatase. We also employed other osteoblast-like cell lines, Saos-2 and MG-63 which expressed ERα as well as ERβ in order to further study the mechanisms of effects of AI on human osteoblasts. We first examined the effects of estradiol (E2), DHT, progesterone (Prg), and AIs described above on cell proliferation of these cell lines, because the status of cell proliferation is important in the maintenance of homeostasis of bone tissue [15]. In addition, the effects of AIs on the conversion ratio of $\Delta_4$ into E2 or testosterone (TST) in hFOB cultured medium were examined. We then screened E2, DHT, and EXE responsive genes using a microarray analysis in these cells, in order to further characterize the possible genomic effects of EXE on cell proliferation of osteoblasts. In this microarray analysis, hFOB was employed in order to examine the effects of E2, DHT, and EXE on native status of human osteoblasts but not on pathological status of osteoblasts such as osteosarcomas.

## Materials and methods

### *Chemicals*

Exemestane (EXE; FCE24304; 6-methyleneandrosta-1,4-diene-3,17-dione) and 17-hydroexemestane (17H-EXE; FCE25071; 6-methyleneandrosta-1,4-diene-17β-ol-3-one) were obtained from Pfizer, Inc. (MI, USA). Aminoglutethimide (AGM) and Aromatase Inhibitor I [AI-I; 4-(Imidazolylmethyl)-1-nitro-9*H*-9-xanthenone] were obtained from Sigma-Aldrich Co. (MO, USA) and EMD Biosciences, Inc. (CA, USA), respectively. Estradiol (E2), progesterone (Prg), and RU38,486 (RU; mifepristone), spironolactone were obtained from Sigma-Aldrich. ICI 182,780 (ICI; fulvestrant) and hydroxyflutamide (OHF) were obtained from Tocris Cookson Inc. (MO, USA) and Toronto Research Chemicals, Inc. (Ontario, Canada), respectively. 5α-dihydrotestosterone (DHT) was obtained from Wako Pure Chemical industries, Ltd. (Osaka, Japan).

Table 1
Aromatase inhibitors used in this study

| | Aminoglutethimide | Exemestane | Aromatase inhibitor I |
|---|---|---|---|
| Trademark [a] | Cytadren® | Aromasin® | – |
| Type [b] | Type II | Type I | Type II |
| Generation | First | Third | – |
| IC50 (nM) [c] | 3000 | 50 | 40 |

[a] Cytadren® is trademark of Novartis Pharmaseutical Corporation. Aromasin® is trademark of Pfizer Inc. Aromatase Inhibitor I is non-clinical compound of Calbiochem®.

[b] Type I is steroidal compound. Type II is a non-steroidal compound.

[c] Refs, Aminoglutethimide and Exemestane are Miller et al. [5]; Aromatase Inhibitor I is Recanatini et al. [14].

These materials were dissolved in pure ethanol (Wako Pure Chemical industries) and serially diluted (final concentrations: $10^{-12}$ M to $10^{-5}$ M), respectively. AGM was dissolved in DMSO (Wako Pure Chemical industries). The final concentration of ethanol and DMSO used in this study did not exceed 0.05%.

### *Osteoblast cell and osteoblast-like cell lines and culture conditions*

Human normal osteoblast cell, hFOB 1.19 cell line (CRL-11372) was obtained from American Type Culture Collection (VA, USA). hFOB 1.19 cell was cultured according to the protocol previously described [16]. The cell line was maintained in a mixture of Dulbecco's Modified Eagle Medium and Ham's F12 medium (1:1) without phenol red (Invitrogen Corporation, CA, USA) supplemented with 10% fetal bovine serum (FBS; JRH Biosciences, KS, USA) and 50 mg/mL G 418 sulfate (EMD Biosciences). Human osteosarcoma cell lines Saos-2 and MG-63 were provided from the Cell Resource Center for Biomedical Research, Tohoku University (Sendai, Japan) and were maintained in a RPMI-1640 (Sigma-Aldrich) with 10% FBS. These cells were pre-incubated for 24 h with FBS-free medium prior to examination in order to remove exo-/endogenous steroid hormones from the culture medium and study the effects of various compounds in the absence of steroids and also to synchronize the cell cycle. Different concentrations of test compounds were added, and the assay was terminated after 3 or 5 days by removing the medium from wells. Steroid blockers were added simultaneously.

### *Characteristics of hFOB, Saos-2, and MG-63*

Expressions of relevant steroid receptors, i.e., ERα, ERβ, and AR were determined using quantitative RT-PCR methods in hFOB, Saos-2, and MG-63 cell lines. mRNA transcripts of steroid synthesis/metabolite enzymes, aromatase, 17β-hydroxysteroid dehydrogenase (17β-HSD) types 1, 2, 3, 4, and 5, and 5α-reductase (5α-Red) types 1 and 2 were all evaluated using RT-PCR methods. The details of quantitative RT-PCR including primer sets employed were previously described in detail [17,18]. Positive controls for these receptors and enzymes were cell lines of human breast cancer, T-47D, and human prostate cancer, LNCaP obtained from Cell Resource Center for Biomedical Research, Tohoku University (Sendai, Japan). Alkaline phosphatase (ALP), an osteoblast-specific marker, was also studied using RT-PCR for characterization of these cell lines.

### *Estradiol and testosterone production assay*

hFOB cells were plated in 10 mm dishes at a density of $10^6$ viable cells and cultured for 48 h. Then media were changed to FBS-free medium, and hFOB cells were incubated with $10^{-7}$ M androstenedione ($\Delta_4$; Sigma-Aldrich) in the presence or absence of EXE or AI-I ($10^{-7}$ M). The media were then collected after 24 h, and E2 and TST were measured by solid-phase radioimmunoassay. Radioimmunoassay was performed in SRL Inc. (Tokyo, Japan) using DPC estradiol kit and DPC total testosterone kit (Diagnostic Products Corporation, LA, USA). In addition, we confirmed that the concentrations of E2 and TST were under the detection limits (E2, 5 pg/mL; TST, 30 pg/mL) in the serum- and phenol red-free medium.

### *Cell proliferation assay*

hFOB, Saos-2, and MG-63 cells were treated with steroids and test compounds for 24, 48, and 72 h, when specimens were harvested and evaluated for cell proliferation using the WST-8 method (Cell Counting Kit-8; Dojindo Inc., Kumamoto, Japan) [18]. Optical densities (OD, 450 nm) were evaluated using a SpectraMax 190 microplate reader (Molecular Devices, Corp., CA, USA) and Softmax Pro 4.3 microplate analysis software (Molecular Devices). The status of proliferation (%) was calculated according to the following equation: (cell OD value after test materials treated/vehicle control cell OD value) × 100.

### *Alkaline phosphatase activity assay*

hFOB, Saos-2, and MG-63 cells were plated in 48 well plate at a density of $10^6$ viable cells and cultured for 48 h. All cell lines were treated with $10^{-9}$ to $10^{-7}$ M exemestane for 72 h, when cells were lysed with 0.05% Triton X-100 (Wako Pure Chemical industries) and evaluated for alkaline phosphatase activity

Table 2
Primer sequences used in quantitative RT-PCR analysis

| cDNA | GB# | Sequence | cDNA position | Size (bp) |
|---|---|---|---|---|
| MYBL2 | NM_002466 | Forward 5′-GTAACAGCCTCACGCCCAAGA-3′<br>Reverse 5′-TCCAATGTGTCCTGTTTGTTCCA-3′ | 1522–1615 | 94 |
| OSTM1 | NM_014028 | Forward 5′-TTGAGAATAAGGCTGAACCTGGAAC-3′<br>Reverse 5′-TTACAGGCACTGTGTCACTGCAAG-3′ | 801–926 | 126 |
| HOXD11* | NM_021192 | Forward 5′-CAC TGT CCT TGG GTT TAA TG-3′<br>Reverse 5′-GGT AAA ATT GTA ACG GGA CG-3′ | 1091–1245 | 174 |
| GPC2 | NM_152742 | Forward 5′-AGA AAT GTG GTC AGC GAA GC-3′<br>Reverse 5′-ACA CCT TCG CAC TGT TTT CC-3′ | 871-1183 | 313 |
| ADCYAP1R1 | NM_001118 | Forward 5′-CAG CAA AAG GGA AAG ACT CG-3′<br>Reverse 5′-GAG CTG CTC TTG CTC AGG AT-3′ | 1351–1584 | 234 |
| COL1A1 | NM_000088 | Forward 5′-GGT GGT GGT TAT GAC TTT GGT T-3′<br>Reverse 5′-CTT GGC TGG GAT GTT TTC AGG T-3′ | 3784–4092 | 309 |
| SMAD1* | NM_005900 | Forward 5′-GGT TCA CCT CAT AAT CCT-3′<br>Reverse 5′-CCT TTG TCA GTT CTC AAT C-3′ | 1779–1887 | 127 |
| SMAD5* | NM_005903 | Forward 5′-AGC TAA AGC CGT TGG ATA-3′<br>Reverse 5′-AGG CAC TAA TAC TGG AGG T-3′ | 668–768 | 119 |
| RUNX2 | NM_004348 | Forward 5′-GTG GAC GAG GCA AGA GTT T-3′<br>Reverse 5′-TAC TGG GAT GAG GAA TGC G-3′ | 782–961 | 198 |
| SPARC | NM_003118 | Forward 5′-CCT GTA CAC TGG CAG TTC-3′<br>Reverse 5′-CCA GGG CGA TGT ACT TGT C-3′ | 793–937 | 163 |
| ALP | NM_000478 | Forward 5′-ACC ATT CCC ACG TCT TCA CA-3′<br>Reverse 5′-AGA CAT TCT CTC GTT CAC CGC C-3′ | 1379–1540 | 162 |
| RPL13A | NM_012423 | Forward 5′-CCT GGA GGA GAA GAG GAA AGA GA-3′<br>Reverse 5′-TTG AGG ACC TCT GTG TAT TTG TCA A-3′ | 487–612 | 126 |

GB#, GeneBank accession number.
All primer sets were designed using OLIGO Primer Analysis Software (TAKARA Bio Inc., Shiga, Japan).
* Forward and reverse primers were located in sama exon.

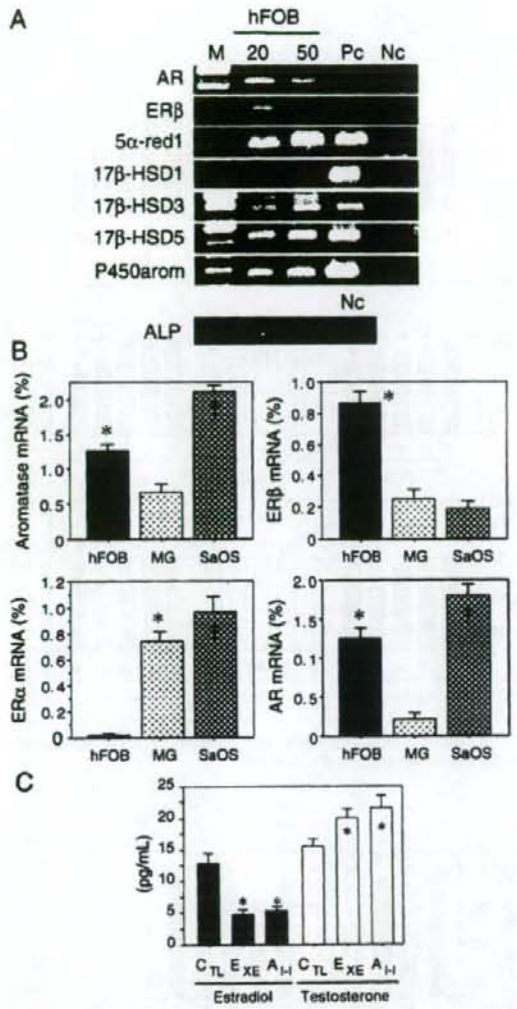


Fig. 2. (A) Results of RT-PCR analysis of steroid hormone receptors and steroid-related enzymes. Both 20 and 50 ng/μL cDNA of hFOB were used for PCR (ALP was 20 ng/μL alone). AR, androgen receptor; ER, estrogen receptor; 5α-red1, 5α-reductase type 1; 17β-HSD, 17β-hydroxysteroid dehydrogenase; P450 arom, aromatase; M, molecular marker; Pc, positive control; Nc, negative control. (B) Expression levels of aromatase, AR, ERα, and ERβ in hFOB, Saos-2, and MG-63. *$p<0.05$ vs. MG-63 (aromatase and AR), vs. MG-63 and vs. Saos-2 (ERβ), vs. hFOB (ERα); †$p<0.05$ vs. hFOB and MG-63 (aromatase and AR), vs. MG-63 and hFOB (ERα). (C) Estradiol and testosterone productions in hFOB cells. The data are expressed as the mean SD ($n=3$). *$p<0.05$ vs. control cells (CTL). EXE, $10^{-7}$ M exemestane; AI-I, $10^{-7}$ M aromatase inhibitor I.

using the *p*-nitrophenylphosphate method (LabAssay ALP; Wako Pure Chemical industries) [19]. Optical densities (OD, 405 nm) were evaluated using a SpectraMax 190 microplate reader (Molecular Devices) and Softmax Pro 4.3 microplate analysis software (Molecular Devices). ALP activity (units/μL)=(concentration of *p*-nitrophenol/15 min)×1 (dilution factor of sample). The ALP activities were presented as units/μL/$10^6$ cells. The ALP activity levels in each case were represented as a ratio of vehicle control (%).

### *Microarray analysis*

The procedure was based on a previously reported study [20]. Cell lysates were prepared using RLT buffer (QIAGEN GmbH, Hilden, Germany). Total RNA was extracted using RNeasy Mini Kit (QIAGEN). First-strand cDNA was synthesized by incubating 5 μg of total RNA with 200 U SuperScript II reverse transcriptase (Invitrogen), 100 pmol T7-(dT)24 primer (Invitrogen). Ten units of T4 DNA polymerase (Invitrogen) were then added, and the dsDNA was mixed with T7 RNA polymerase (Invitrogen). The purified cRNA was fragmented at 300–500 bp as target solution. Hybridization was performed with the GeneChip Human Genome 133 ver. 2.0 (Affymetrix, Inc., CA, USA). The reacted arrays were then scanned as digital image files and scanned data were analyzed with GeneChip software (Affymetrix). Relative levels of gene expression were calculated by global normalization.

Data were subjected to hierarchical clustering analysis and visualization using the Cluster and TreeView programs (Stanford University) in order to generate tree structures based on the degree of similarity, as well as matrices comparing the levels of expression of individual genes in each sample [21].

### *Real-time PCR*

Real-time PCR was carried out using the LightCycler System and the FastStart DNA Master SYBR Green I (Roche Diagnostics GmbH, Mannheim, Germany). The primer sequences used in this study are summarized in Table 2. An initial denaturing step of 95 °C for 10 min was followed by 35 cycles, respectively, at 95 °C for 10 min; 15 s annealing at 65 °C (ALP, COL1A1), 64 °C (MYBL2, OSTM1, RPL13A), 62 °C (SMAD1, SMAD5, SPARC, RUNX2), or 60 °C (HOXD11); and extension for 15 s at 72 °C. Negative control experiments included those lacking cDNA substrates to confirm the presence of exogenous contaminant DNA. No amplified products were detected under these conditions. The mRNA levels in each case were represented as a ratio of RPL13A (%) [22].

### *Immunohistochemistry of AR*

Five non-pathological bone tissues were retrieved from surgical pathology files (two females and three males, 17 to 55 years old) of Department of Pathology, Tohoku University Hospital (Sendai, Japan).

Tissue sections were immunostained using a biotin-streptavidin method with Histofine kit (Nichirei Co. Ltd., Tokyo, Japan). The monoclonal antibody for AR (AR411) [23] was obtained from DakoCytomation (Kyoto, Japan). Experimental procedures employed in our present study have been previously described in detail [22,23]. The dilutions of primary AR antibody were 1:100. The antigen-antibody complex was then visualized with 3,3′-diaminobenzidine solution, and counterstained with hematoxylin. Prostate cancer was used as a positive control for AR. Normal mouse IgG was used as a negative control for immunostaining and no specific immunoreactivity was detected.

### *Statistical analysis*

Results were expressed as mean±SD. Statistical analysis was performed with the StatView 5.0 J software (SAS Institute Inc., NC, USA). All data were analyzed by analysis of variance (ANOVA) followed by post hoc Bonferroni/Dunnett multiple comparison test. A $p$-value$<0.05$ was considered to indicate statistical significance.

## Results

### *Characteristics of hFOB, MG-63, and Saos-2 cell line*

Characteristics of osteoblast and osteoblast-like cell lines are summarized in Figs. 2A and B. hFOB cells expressed mRNA transcripts of AR and ERβ. Relatively low level of ERα mRNA transcript was detected in hFOB cells. Aromatase, 17β-HSD type 1, 3, and 5, and 5α-Red types 1 and 2 mRNA transcripts were all detected in hFOB cells by

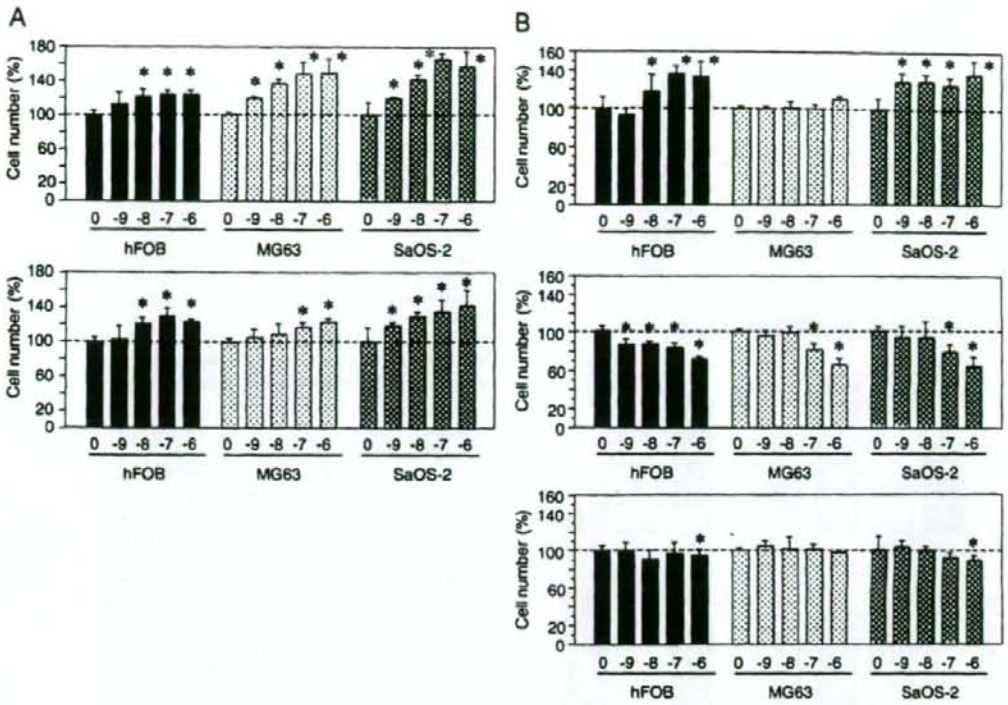


Fig. 3. (A) Proliferation of hFOB cells treated by estradiol (top) and 5α-DHT (bottom). *$p<0.05$ vs. vehicle control (0). (B) Proliferation of hFOB cells treated by exemestane (top), aminogluthetimide (middle), and Aromatase Inhibitor-I (bottom). *$p<0.05$ vs. vehicle control (0). $n=5$.

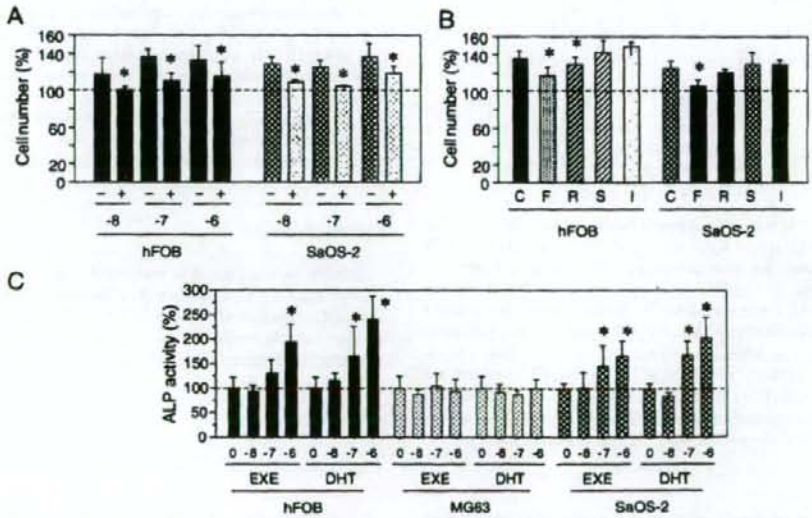


Fig. 4. (A) Effects of hydroxyflutamide on exemestane ($10^{-8}$ to $10^{-6}$ M) stimulated the cell proliferation of both hFOB and Saos-2. With (+) or without (−) hydroxyflutamide, $p<0.05$ vs. without hydroxyflutamide (*). (B) Effects of steroid receptor blockers on exemestane ($10^{-7}$ M) stimulated cell proliferation of hFOB and Saos-2. C, $10^{-7}$ M exemestane; F, hydroxyflutamide ($5\times10^{-6}$ M); R, RU38,486 ($5\times10^{-6}$ M); S, spironolactone ($5\times10^{-6}$ M); I, ICI182,720 ($5\times10^{-6}$ M). *$p<0.05$ vs. C (C) ALP activity in hFOB, Saos-2, MG-63 treated with exemestane (EXE, $10^{-8}$ to $10^{-6}$ M), or 5α-DHT (DHT, $10^{-8}$ to $10^{-6}$ M). *$p<0.05$ vs. vehicle control (0).

RT-PCR. Aromatase, ERα, ERβ, and AR were all detected in osteoblast-like cell lines, Saos-2 and MG-63 (Fig. 2B). In hFOB cell, expression of ERβ mRNA was more predominant than that of ERα mRNA. ERα mRNA as well as ERβ mRNA was detected in Saos-2 and MG-63 cells. The levels of AR mRNA expression in both hFOB and Saos-2 were significantly higher ($p=0.01$) than that in MG-63. ALP mRNA was also detected in intact hFOB, Saos-2, and MG-63 cells (data not present), respectively.

*Estradiol and testosterone production*

Results were summarized in Fig. 2C. The E2 levels in the medium of hFOB supplemented with $\Delta_4$ treated with EXE or AI-I were significantly lower than that of cells without AIs. The levels of TST in the medium of hFOB supplemented with $\Delta 4$ treated with EXE or AI-I were significantly higher than that of cells without AIs.

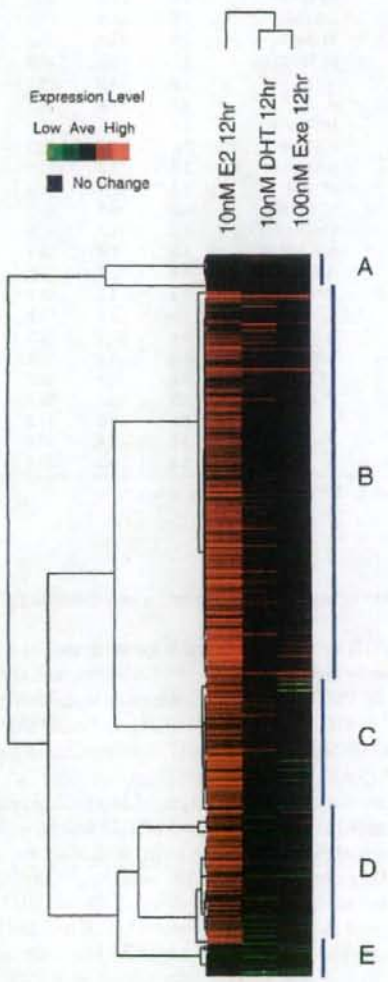


Fig. 5. In clustering analysis of the expression levels of each gene in hFOB cells treated with estradiol (E2), 5α-dihydrotestosterone (DHT), and exemestane (Exe).

*Cell proliferation*

Results of the cell proliferation assays are summarized in Figs. 3 and 4. There was a significant increment in the number of the cells after 72 h in hFOB, Saos-2, and MG-63 cells treated with $10^{-9}$ M (Saos-2 and MG-63) or $10^{-8}$ M (hFOB) to $10^{-6}$ M E2 (Fig. 3A). The cell number of hFOB and Saos-2 cells treated by $10^{-9}$ M (Saos-2) or $10^{-8}$ M (hFOB) to $10^{-6}$ DHT for 72 h was also significantly higher than control (Fig. 3A). The number of MG-63 cells was significantly increased only by high dose of DHT ($10^{-7}$ M and $10^{-6}$ M) treatments (Fig. 3A). Prg ($10^{-9}$ M to $10^{-6}$ M) treatments did not change the number of cells even after 72 h in all three cell lines examined (data not present).

Both EXE (Fig. 3B) and 17H-EXE (data not present) treatments of $10^{-8}$ M to $10^{-6}$ M, which were comparable to pharmacological inhibition doses of aromatization (Table 1), significantly increased the hFOB cell number for 72 h, respectively. In Saos-2 cells treated with relatively low dose, $10^{-9}$ to $10^{-6}$ M EXE, there was a significant increment in the number of the cells after 72 h (Fig. 3B). However, all the dose ($10^{-9}$ M to $10^{-6}$ M) of EXE employed did not results in the change of cell number of MG-63 even after 72 h of treatment (Fig. 3B). The cell number of both hFOB and Saos-2 cells treated by both $10^{-6}$ M EXE and/or 17H-EXE for 48 h was also significantly higher than that treated for 24 h (data not present).

AGM treatment [$10^{-9}$ (hFOB) or $10^{-7}$ (Saos-2 and MG-63) to $10^{-6}$ M] diminished the number of these three cells (Fig. 3B) and morphological changes in these cells were consistent with those caused by cytotoxic effects (data not present). AI-I treatment ($10^{-9}$ to $10^{-7}$ M) was not associated with significant increment of the cell number in these cell lines (Fig. 3B). Only high dose ($10^{-6}$ M) of AI-I significantly diminished the cell numbers of hFOB and Saos-2 but not of MG-63 (Fig. 3B).

The androgen receptor antagonist OHF ($5\times10^{-6}$ M) diminished the effects of EXE on these increments of both hFOB and Saos-2 cells (Figs. 4A and B). Treatment with RU but not spironolactone and ICI also inhibited EXE effects on hFOB cells (Fig. 4B).

*ALP activity assay*

Results of the ALP activity assay were summarized in Fig. 4C. There was a significant increment in the ALP activity of both hFOB and Saos-2 cells treated with $10^{-7}$ M (Saos-2) and/or $10^{-6}$ M (hFOB and Saos-2) EXE. Both $10^{-7}$ M and $10^{-6}$ M DHT treatment also increased the ALP activity in hFOB and Saos-2 cells, respectively. There were no changes of ALP activity in MG-63 treated with $10^{-8}$ M to $10^{-6}$ M of EXE and DHT, respectively.

Table 3a
Genes induced by exemestane treatment in hFOB cells—2.0 higher

| | Gene title | Gene symbol | Raw data | | | Ratio | |
|---|---|---|---|---|---|---|---|
| | | | C | D | Ex | D | Ex |
| NM_002466 | V-myb myeloblastosis viral oncogene homolog (avian)-like 2 | **MYBL2** | 70.9 | 156.9 | 150.3 | 2.2 | 2.1 |
| AW444985 | – | – | 57.8 | 124.7 | 127.1 | 2.2 | 2.2 |
| AF143684 | Myosin IXB | MYO9B | 48.3 | 64.4 | 122.2 | 1.3 | 2.5 |
| NM_024682 | TBC1 domain family, member 17 | TBC1D17 | 31.7 | 37.6 | 64.8 | 1.2 | 2.0 |
| BE965311 | Chromosome 16 open reading frame 23 | C16orf23 | 29.2 | 44.2 | 64.0 | 1.5 | 2.2 |
| NM_004233 | CD83 antigen (activated B lymphocytes, immunoglobulin superfamily) | CD83 | 29.0 | 66.5 | 60.9 | 2.3 | 2.1 |
| AI806031 | Skeletal muscle and kidney enriched inositol phosphatase | SKIP | 27.7 | 48.6 | 55.4 | 1.8 | 2.0 |
| AL136729 | Ring finger protein 123 | RNF123 | 20.0 | 23.7 | 41.3 | 1.2 | 2.1 |
| NM_015254 | Kinesin family member 13B | KIF13B | 13.0 | 24.5 | 39.4 | 1.9 | 3.0 |
| AL110249 | Chromosome 20 open reading frame 194 | C20orf194 | 13.4 | 39.0 | 29.7 | 2.9 | 2.2 |
| AF208502 | Early B-cell factor | EBF | 12.5 | 21.1 | 28.5 | 1.7 | 2.3 |
| AW007221 | Solute carrier family 13 (sodium/sulfate symporters), member 4 | SLC13A4 | 12.3 | 9.6 | 27.8 | 0.8 | 2.3 |
| AB007458 | TP53 activated protein 1 | TP53AP1 | 12.6 | 22.2 | 26.2 | 1.8 | 2.1 |
| AV713913 | Osteopetrosis associated transmembrane protein 1 | **OSTM1** | 9.8 | 16.5 | 21.3 | 1.7 | 2.2 |
| BF339201 | THAP domain containing 6 | THAP6 | 6.0 | 14.0 | 20.6 | 2.3 | 3.4 |
| AK000455 | Hypothetical gene MGC16733 similar to CG12113 | MGC16733 | 7.3 | 16.6 | 18.8 | 2.3 | 2.6 |
| AW974816 | – | – | 2.2 | 16.0 | 17.2 | 7.2 | 7.7 |
| AK025325 | Transcribed locus, moderately similar to NP_689573.2 zinc finger protein 573 | – | 7.3 | 11.4 | 16.2 | 1.6 | 2.2 |
| NM_021192 | Homeo box D11 | **HOXD11** | 5.3 | 16.2 | 15.8 | 3.0 | 3.0 |
| NM_022169 | ATP-binding cassette, sub-family G (WHITE), member 4 | ABCG4 | 7.0 | 10.5 | 15.7 | 1.5 | 2.2 |
| R62907 | Disabled homolog 2, mitogen-responsive phosphoprotein (*Drosophila*) | DAB2 | 7.7 | 13.0 | 15.5 | 1.7 | 2.0 |
| NM_002661 | Phospholipase C, gamma 2 (phosphatidylinositol-specific) | PLCG2 | 7.3 | 12.3 | 15.3 | 1.7 | 2.1 |
| BG393032 | Solute carrier family 13 (sodium/sulfate symporters), member 4 | SLC13A4 | 6.4 | 6.7 | 15.1 | 1.0 | 2.3 |
| BC002794 | Tumor necrosis factor receptor superfamily, member 14 | TNFRSF14 | 6.2 | 11.3 | 13.6 | 1.8 | 2.2 |
| BC042908 | KIAA0690 | KIAA0690 | 5.6 | 7.4 | 13.5 | 1.3 | 2.4 |
| AW451961 | Adenylate cyclase activating polypeptide 1 (pituitary) receptor type I | **ADCYAP1R1** | 4.3 | 11.7 | 13.2 | 2.7 | 3.1 |
| AI863264 | Glypican 2 (cerebroglycan) | **GPC2** | 5.3 | 7.2 | 13.2 | 1.3 | 2.5 |
| AF130050 | ACA47 scaRNA gene | - | 5.6 | 9.5 | 12.9 | 1.7 | 2.3 |
| AK022326 | Hypothetical gene supported by AK022326 | - | 6.1 | 12.7 | 12.9 | 2.1 | 2.1 |
| AK021807 | Low density lipoprotein receptor-related protein 11 | LRP11 | 5.9 | 6.2 | 12.8 | 1.0 | 2.2 |
| AU155415 | Kallikrein 7 (chymotryptic, stratum corneum) | KLK7 | 5.6 | 13.5 | 12.7 | 2.4 | 2.3 |
| BF673779 | Hypothetical protein FLJ30834 | FLJ30834 | 5.5 | 6.3 | 12.3 | 1.1 | 2.2 |
| AV646335 | – | – | 2.6 | 13.0 | 11.2 | 5.0 | 4.3 |
| BC040600 | – | – | 5.0 | 5.4 | 10.6 | 1.1 | 2.1 |
| AI131035 | – | – | 5.1 | 9.2 | 10.5 | 1.8 | 2.1 |

C, vehicle control; D, 5α-dihydrotestosterone; Ex, exemestane. Genes that performed quantitative RT-PCR were described in bold style.

*Microarray/clustering analysis*

In hFOB cells, the hierarchical clustering analysis contains 430 genes which demonstrated expression ratios above 2.0-fold and below 0.5-fold compared with vehicle control cells after 12 h of each gene treated with $10^{-8}$ M E2, $10^{-8}$ M DHT, or $10^{-7}$ M EXE. The expression profiles of EXE treated cells were closely related to those of DHT (Fig. 5). In this study, we focused on 35 genes (Table 3a), which were all up-regulated twice or more than control. In this group, we further focused on 5 genes, B-Myb 2 (MYBL2), osteopetrosis associated transmembrane protein 1 (OSTM1), homeo box D 11 (HOXD11), adenylate cyclase activating polypeptide 1 receptor (ADCYAP1R1), and glypican 2 (GPC2) which are all considered to play important roles in EXE or DHT induced cell proliferation. We therefore examined whether these 5 genes were increased by EXE or DHT treatments using quantitative RT-PCR in hFOB cells. We also examined the validation of results of microarray analysis obtained in hFOB cells in Saos-2 and MG-63 cells.

*Validation of microarray analysis using quantitative RT-PCR*

In hFOB cells, all of these 5 genes described above were significantly increased by $10^{-7}$ M EXE treatment, and 3/5 genes (except for OSTM1 and GPC2) were also significantly increased by $10^{-8}$ M DHT treatment. HOXD11 and ADCYAP1R1 genes increased by both EXE and DHT were significantly diminished by OHF ($5\times10^{-6}$ M) treatment (Figs. 6A–C).

The similar results of changes of MYBL2 expression were also obtained in both Saos-2 and MG-63 treated with EXE and DHT, respectively (Fig. 6A). In addition, the results of HOXD11 expression in hFOB were equivalent to those in Saos-2 but not in MG-63 treated with EXE and DHT (Fig. 6B). Other genes induced by treatment of EXE and DHT in hFOB such as OSTM1, GPC2, and ADCYAP1R1 were not changed in both Saos-2 and MG-63 cells treated with EXE and DHT, respectively (data not present). AI-I or AGM treatment did not increase all of these genes expression in hFOB (data not present).

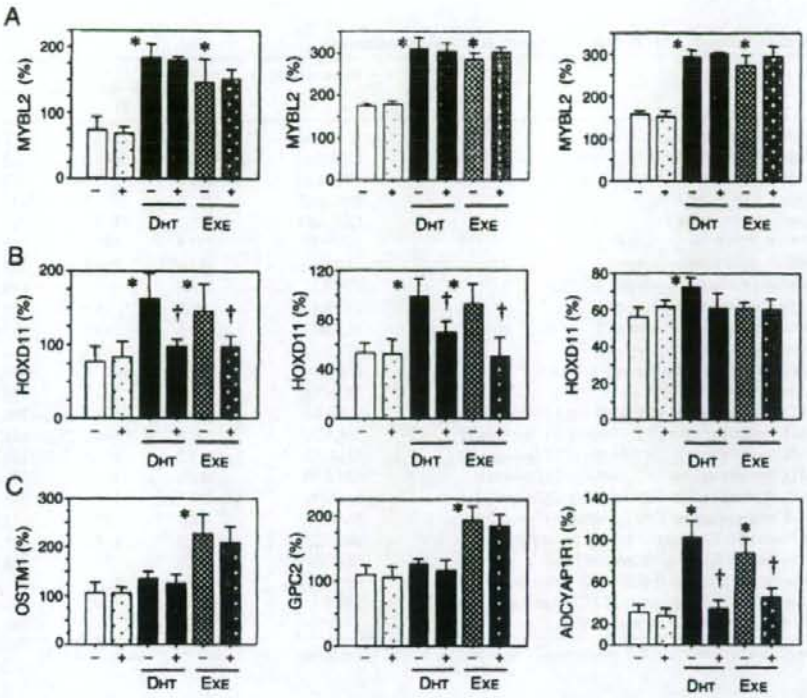


Fig. 6. Validation of microarray analysis. (A) Expression levels of MYBL2 in hFOB (left), Saos-2 (middle), and MG-63 (right). (B) Expression levels of HOXD11 in hFOB (left), Saos-2 (middle), and MG-63 (right). (C) Expression levels of OSTM1, GPC2, and ADCYAP1R1 in hFOB. DHT: $10^{-8}$ M 5α-dihydrotestosterone, EXE: $10^{-7}$ M Exemestane, with (+) or without (−) hydroxyflutamide, $p<0.05$ vs. control (*) or without hydroxyflutamide (†).

*Analysis of osteoblast growth-related genes*

Results of microarray analysis in hFOB cell demonstrated that osteoblast growth-related genes [24,25] such as COL1A1, SMAD1, SMAD5, SPARC, and RUNX2 were all up-regulated by exemestane ($10^{-7}$ M) treatment but the degrees of increment were all under 2-fold (Table 3b). In this microarray analysis, other expression levels of previously reported osteoblast-related genes were not altered.

In hFOB cells, the validation analysis of these genes described above using quantitative RT-PCR (Fig. 7) demonstrated that 4/5 genes (except for COL1A1) were significantly increased by $10^{-7}$ M EXE treatment, and 4/5 genes (except for SMAD1) were also significantly increased by $10^{-8}$ M DHT treatment. The increased expression of the SMAD1, SMAD5, and SPARC genes by EXE or DHT, was significantly diminished by OHF ($5\times10^{-6}$ M) treatment. There were no effects of OHF pretreatment on the increased expression levels of RUNX2 that had occurred after both EXE and DHT treatments. Both AI-I and AGM treatment could not increase all of these genes expression in hFOB (data not present).

In Saos-2 cells, 4/5 genes (except for RUNX2) were significantly increased by $10^{-7}$ M EXE treatment, and 3/5 genes (except for RUNX2 and SMAD1) were also significantly increased by $10^{-8}$ M DHT treatment. The increment of the COL1A1, SMAD5, and SPARC genes expression by EXE or DHT, was significantly diminished by OHF ($5\times10^{-6}$ M) treatment. All of these 5 genes did not change in MG-63 cells treated with EXE or DHT, respectively (data not present).

*Immunohistochemistry of AR*

Marked AR immunoreactivity was detected in the nuclei of osteoblasts or lining cells but not in osteoclasts in four cases (Fig. 8). In these four cases, AR immunoreactivity was also detected in osteocytes and condrocytes. In one case, there was no immunoreactivity in all types of bone cells.

## Discussion

In the clinical study of EXE compared to placebo administrated for two years [26,27], EXE modestly enhanced bone loss from the femoral neck without significant influence on lumber bone loss despite a marked systemic estrogen depletion. Furthermore, the risks of clinical bone fractures are considered to be lower with EXE treatment than that seen with non steroidal AIs [27,28], though it is also important to recognize that EXE has not been shown to significantly increase the amount of bone mass in various clinical studies of breast cancer patients [26,27]. The relative protective effect of EXE, a

Table 3b
Genes induced by exemestane treatment in hFOB cells—the osteoblast growth-related genes

| | Gene title | Gene symbol | Raw data | | | Ratio | |
|---|---|---|---|---|---|---|---|
| | | | C | D | Ex | D | Ex |
| K01228 | Collagen, type I, alpha 1 | **COL1A1** | 2797.2 | 3240.9 | 3058.5 | 1.2 | 1.1 |
| BE221212 | Collagen, type I, alpha 1 | **COL1A1** | 2741.1 | 3048.3 | 3052.2 | 1.1 | 1.1 |
| AI743621 | Collagen, type I, alpha 1 | **COL1A1** | 228.0 | 241.6 | 242.5 | 1.1 | 1.1 |
| AA788711 | Collagen, type I, alpha 2 | COL1A2 | 2250.6 | 2474.3 | 2375.4 | 1.1 | 1.1 |
| NM_000089 | Collagen, type I, alpha 2 | COL1A2 | 1749.1 | 1848.7 | 1787.6 | 1.1 | 1.0 |
| M60485 | Fibroblast growth factor receptor 1 | FGFR1 | 178.9 | 185.7 | 198.6 | 1.0 | 1.1 |
| BE467261 | Fibroblast growth factor receptor 1 | FGFR1 | 165.4 | 208.6 | 189.7 | 1.3 | 1.1 |
| M63889 | Fibroblast growth factor receptor 1 | FGFR1 | 119.3 | 111.6 | 140.5 | 0.9 | 1.2 |
| NM_023110 | Fibroblast growth factor receptor 1 | FGFR1 | 60.5 | 84.0 | 70.2 | 1.4 | 1.2 |
| AU145411 | Fibroblast growth factor receptor 1 | FGFR1 | 29.2 | 44.1 | 37.5 | 1.5 | 1.3 |
| AI359368 | Fibroblast growth factor receptor 3 | FGFR3 | 41.4 | 65.5 | 58.7 | 1.6 | 1.4 |
| NM_001552 | Insulin-like growth factor binding protein 4 | IGFBP4 | 809.1 | 1027.5 | 1040.4 | 1.3 | 1.3 |
| AL353944 | Runt-related transcription factor 2 | **RUNX2** | 192.9 | 226.3 | 216.3 | 1.2 | 1.1 |
| AU146891 | SMAD, mothers against DPP homolog 1 (*Drosophila*) | **SMAD1** | 161.2 | 195.6 | 204.6 | 1.2 | 1.3 |
| NM_005901 | SMAD, mothers against DPP homolog 2 (*Drosophila*) | SMAD2 | 100.3 | 108.2 | 113.7 | 1.1 | 1.1 |
| NM_005902 | SMAD, mothers against DPP homolog 3 (*Drosophila*) | SMAD3 | 110.2 | 106.5 | 127.7 | 1.0 | 1.2 |
| BF526175 | SMAD, mothers against DPP homolog 5 (*Drosophila*) | **SMAD5** | 361.0 | 488.3 | 514.2 | 1.4 | 1.4 |
| AI478523 | SMAD, mothers against DPP homolog 5 (*Drosophila*) | SMAD5 | 300.7 | 384.9 | 346.9 | 1.3 | 1.2 |
| AF010601 | SMAD, mothers against DPP homolog 5 (*Drosophila*) | SMAD5 | 79.2 | 99.7 | 87.6 | 1.3 | 1.1 |
| AY014180 | SMAD-specific E3 ubiquitin protein ligase 2 | SMURF2 | 804.2 | 844.7 | 851.8 | 1.1 | 1.1 |
| AU157259 | SMAD-specific E3 ubiquitin protein ligase 2 | SMURF2 | 77.1 | 81.5 | 86.3 | 1.1 | 1.1 |
| AL575922 | Secreted protein, acidic, cysteine-rich (osteonectin) | **SPARC** | 1702.1 | 1935.5 | 1925.8 | 1.1 | 1.1 |
| BF508662 | Sprouty homolog 1, antagonist of FGF signaling (*Drosophila*) | SPRY1 | 31.9 | 46.3 | 45.4 | 1.5 | 1.4 |
| NM_014886 | TGF beta-inducible nuclear protein 1 | TINP1 | 1185.7 | 1259.5 | 1241.1 | 1.1 | 1.0 |

C, vehicle control; D, 5α-dihydrotestosterone; Ex, exemestane. Genes that performed quantitative RT-PCR were described in bold style.

steroidal aromatase inhibitor, has been therefore attributed to its actions through AR in osteoblasts. Systemic androgenic effects such as hypertricosis, hair loss, hoarseness, and acne have been reported only in 4% [6] of the patients treated with EXE (25 mg/day) and the frequency of these effects increases to approximately 10% in those treated with higher dose 200 mg/day of EXE [6]. This finding suggests that the patients treated with EXE are under relatively weak systemic androgenic effects. Androgen sensitivity has been well-known to be subject to great individual variation caused by AR gene CAG polymorphism in women as well as men [29,30]. Therefore, this 5 to 10% of the patients who manifested clinical androgenic effects by EXE treatment may be individuals associated with relatively enhanced androgenic sensitivity. Replacement therapy with TST is generally effective at restoring bone in hypogonadal men [31]. In female-to-male, genetic female transsexual subjects, high-dose TST therapy generally increased BMD at the femoral neck, despite decrement of E2 to postmenopausal levels [32,33]. Therefore, androgens may play an important role in bone protection in women as well as men.

The results of cell proliferation assay demonstrated that the cell number of MG-63 was increased by both E2 and DHT treatments, but the dose of DHT was relatively higher than that in two other cells. MG-63 expressed higher levels of ERα/β mRNA, but the level of AR mRNA was lower than that in both Saos-2 and hFOB. Both cell proliferation and ALP activity of MG-63 could not be stimulated by EXE treatment. Molecular mechanisms of androgen actions on osteoblasts have remained largely unknown. Androgen is well-known to stimulate osteoblast proliferation [34] and differentiation [35]. For instance, osteoprotegerin mRNA was increased by TST as well as DHT treatments in mouse 3T3-E1 cells [36].

AR and ERβ but not ERα are predominantly detected in osteoblasts located on human cancellous bone using immunohistochemical analysis [37]. Therefore, hFOB examined in this study is considered to maintain relatively native status of sex steroids pathways in human osteoblasts. Therefore, we employed hFOB for further examination of EXE effects on osteoblast gene expression pattern using microarray analysis. In this study, we demonstrated that the genes MYBL2 [38], OSTM1 [39], HOXD11 [40], ADCYAP1R1 [41], and GPC2 [42] were target genes of EXE alone or both EXE and DHT in hFOB using microarray/PCR analysis. These genes were demonstrated to be involved in regulation of cell cycle, differentiation, and transcription. In EXE or DHT treatment in hFOB and Saos-2, in which cells proliferations were stimulated, an increased expression of HOXD11 gene was detected. The product of the mouse Hoxd11 gene was reported to play a role in forelimb morphogenesis [40,43]. Therefore, these finding suggest that osteoblast cell proliferation stimulated by EXE treatment may depend on HOXD11 gene expression through AR. In this study, the cell proliferation of MG-63, which expressed relatively low level of AR, was not stimulated by EXE. In addition, HOXD11 gene expression was not up-regulated by EXE treatment in MG-63 cells. These results were also consist with the protective effects of EXE through potential androgen-HOXD11 pathway in osteoblast cells. In this study, we also examined the effects of EXE and DHT on osteoblast growth-related genes using micro-

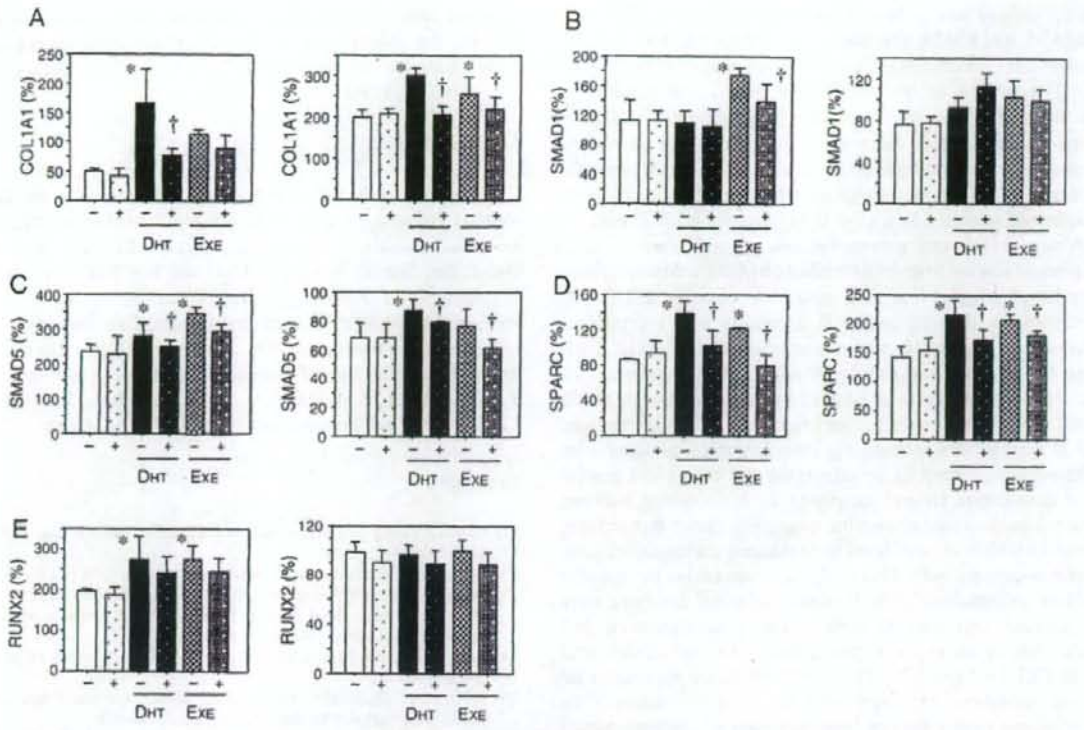


Fig. 7. Expression levels of osteoblast growth-related genes in hFOB (left) and Saos-2 (right). DHT: $10^{-8}$ M 5α-dihydrotestosterone, EXE: $10^{-7}$ M Exemestane, with (+) or without (−) hydroxyflutamide, $p<0.05$ vs. control (*) or without hydroxyflutamide (†).

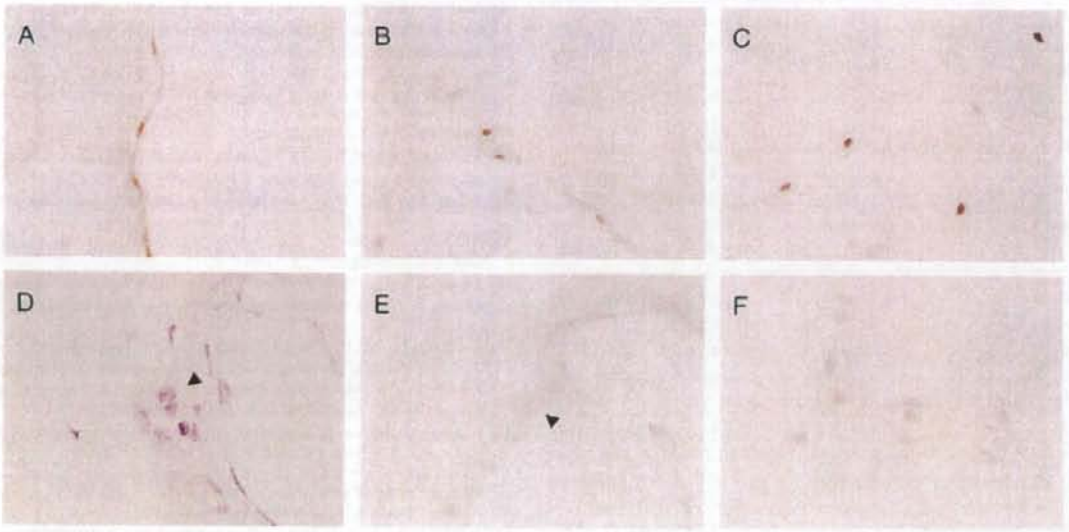


Fig. 8. Immunohistochemistry of androgen receptor in human bone tissues. Immunoreactivity of androgen receptor was detected in nuclei of osteoblasts/liner cells (A, B) but not in osteoclasts (D, E; arrowheads). Immunoreactivity of androgen receptor was also detected in nuclei of osteocytes (C) and condrocytes (F).

array analysis and following quantitative RT-PCR. COL1A1, SMAD5, and SPARC (osteonectine) were up-regulated by EXE and/or DHT treatments in both hFOB and Saos-2 cells. EXE or DHT treatments in both hFOB and Saos-2 also resulted in increased ALP activity. There have been, however, no studies reported on whether these genes are primary or secondary androgen responsive genes in osteoblasts. The AR-specific antagonist, OHF demonstrated no inhibitory effects on RUNX2 expression increased by EXE or DHT treatment in hFOB cells. In addition, hFOB cell growth induced by high dose of EXE treatment was not completely inhibited by OHF treatment. These results all suggest that EXE also may stimulate hFOB cell proliferation through both AR dependent and independent pathways. From our data of steroid production in hFOB, EXE may have an additional androgenic effect through increased TST levels in conjunction with inhibition of aromatization in hFOB cells. However, it awaits further investigations for clarification.

In normal bone remodeling, bone formation by osteoblasts follows bone resorption by osteoclasts and occurs in a precise and quantitative manner (coupling). In this coupling between bone formation and resorption, a coupling factor that induces bone formation is considered to be released during osteoclastic bone resorption [44]. This study has focused on the specific effects on osteoblast cells. However, it is true that there were significant increases in both serum bone formation and resorption markers in postmenopausal women administered with EXE for 2 years [26]. Osteoclasts, which are responsible for bone resorption, are target cells for many anti-osteoporosis therapeutic agents such as bisphosphonate of postmenopausal women [45]. However, it is unclear whether EXE acts on osteoclast directly. Chen et al. [46] reported that testosterone inhibited osteoclast formation stimulated by parathyroid hormone through the AR but not through the production of intrinsic estrogen using primary mouse osteoclast cells. In both human and rodent bone tissues, AR is expressed in both osteoblasts and osteocytes [47,48]. However, AR is detected in osteoclasts of rodent but not in human cells [31,47,48]. Therefore, in humans, androgens are considered to exert their effects on bone through osteoblasts. EXE may therefore exert its possible androgenic effects on human bone through osteoblasts but not osteoclasts. Results of our present study also suggest the possible roles of EXE on osteoblast cells through AR independent manner. Results of clinical studies suggest that the combination therapy of AI and COX-2 inhibitors could provide more effective aromatase inhibition than single therapy in hormone-sensitive postmenopausal breast cancer [49]. Bone resorption induced by IL-1 and IL-6 was also reported to occur via stimulation of COX-2 dependent $PGE_2$ production in osteoblasts *in vitro* [50]. Therefore, further investigations are required to clarify the effects of AI including EXE on human bone tissues.

In summary, this study using osteoblast and osteoblast-like cell lines suggested the potential protective effect of steroidal AI, EXE on osteoblasts occurred through both AR dependent and independent pathways. HOXD11 gene known as bone morphogenesis factor and osteoblast growth-related genes were induced by EXE treatment as well as DHT treatment in both hFOB and Saos-2. Damages of bone tissues by estrogen depletion caused by AI administration are considered unavoidable but the selection of potential hormone therapies which could minimize the damages or injuries of bone tissues is considered important.

## Acknowledgments

We appreciate Dr. Shin-ichi Hayashi (Divisions of Molecular Medical Technology, Tohoku University School of Medicine) for critical comments. We also appreciate Ms. Chika Tazawa, Ms. Toshie Suzuki, Ms. Miki Mori and Mr. Katsuhiko Ono (Department of Pathology, Tohoku University School of Medicine) for skillful technical assistances. This research was supported by Grant-in-aid for Health and Labor Sciences Research Grant on Risk of Chemical Substances (H16-Kagaku-002) from Ministry of Health, Labor, and Welfare, Japan and Kanzawa Medical Research Foundation, Nagano, Japan.

## References

[1] Rogers J. Estrogens in the menopause and postmenopause. N Engl J Med 1969;280:364–7.
[2] Wingate L. The epidemiology of osteoporosis. J Med 1984;15:245–66.
[3] Felson DT, Zhang Y, Hannan MT, Kiel DP, Wilson PW, Anderson JJ. The effect of postmenopausal estrogen therapy on bone density in elderly women. N Engl J Med 1993;329:1141–6.
[4] Lester L, Coleman R. Bone loss and the aromatase inhibitors. Br J Cancer 2005;93:S16–22.
[5] Miller WR, Dixon JM. Antiaromatase agents: preclinical data and neoadjuvant therapy. Clin Breast Cancer 2000;1:S9–S14.
[6] Lønning PE, Paridaens R, Thurlimann B, Piscitelli G, di Salle E. Exemestane experience in breast cancer treatment. J Steroid Biochem Mol Biol 1997;61:151–5.
[7] Center for Drug Evaluation and Research Application Number NDA 20753 (Exemestane) Medical Review. Food and Drug Administration, 1999.
[8] Goss PE, Qi S, Josse RG, Pritzker KPH, Mendes M, Hu H, et al. The steroidal Aromatase inhibitor exemestane prevent bone loss in ovariectomized rats. Bone 2004;34:384–92.
[9] Goss PE, Qi S, Cheung AM, Hu H, Mendes M, Pritzker KPH. Effects of steroidal aromatase inhibitor exemestane and the nonsteroidal aromatase inhibitor letrozole on bone and lipid metabolism in the ovariectomized rats. Clin Cancer Res 2004;10:5717–23.
[10] Sasano H, Uzuki M, Sawai T, Nagura H, Matsunaga G, Kashimoto O, et al. Aromatase in human bone tissue. J Bone Miner Res 1997;12:1416–23.
[11] Schweikert HU, Wolf L, Romalo G. Oestrogen formation from Androstendione in human bone. Clin Endocrinol 1995;43:37–42.
[12] Purohit A, Flanagan AM, Reed MJ. Estrogen synthesis by osteoblast cell lines. Endocrinology 1992;131:2027–9.
[13] Tanaka S, Haji M, Nishi Y, Yanase T, Takayanagi R, Nawata H. Aromatase activity in human osteoblast-like osteosarcoma cell. Calcif Tissue Int 1993;52:107–9.
[14] Recanatini M, Bisi A, Cavalli A, Belluti F, Gobbi S, Rampa A, et al. A new class of nonsteroidal aromatase inhibitors: design and synthesis of chromone and xanthone derivatives and inhibition of the P450 enzymes aromatase and 17 alpha-hydroxylase/C17,20-lyase. J Med Chem 2001;44:672–80.
[15] Linkhart TA, Mohan S, Baylink DJ. Growth factors for bone growth and repair: IGF, TGF beta and BMP. Bone 1996;19:1S–12S.
[16] Harris SA, Enger RJ, Riggs BL, Spelsberg TC. Development and characterization of a conditionally immortalized human fetal osteoblastic cell line. J Bone Miner Res 1995;10:178–86.
[17] Suzuki T, Darnel AD, Akahira JI, Ariga N, Ogawa S, Kaneko C, et al. 5alpha-reductases in human breast carcinoma: possible modulator of in situ androgenic actions. J Clin Endocrinol Metab 2001;86:2250–7.

[18] Miki Y, Suzuki T, Tazawa C, Ishizuka M, Semba S, Gorai I, et al. Analysis of gene expression induced by diethylstilbestrol (DES) in human primitive Müllerian duct cells using microarray. Cancer Lett 2005;220:197–210.
[19] Yamamoto M, Takahashi Y, Tabata Y. Controlled release by biodegradable hydrogels enhances the ectopic bone formation of bone morphogenetic protein. Biomaterials 2003;24:4375–83.
[20] Kanno J, Aisaki K, Igarashi K, Nakatsu N, Ono A, Kodama Y, et al. "Per cell" normalization method for mRNA measurement by quantitative PCR and microarrays. BMC Genomics 2006;29:64.
[21] Eisen MB, Spellman PT, Brown PO, Bostein D. Cluster analysis and display of genome-wide expression patterns. Proc Natl Acad Sci U S A 1998;95:14863–8.
[22] Miki Y, Nakata T, Suzuki T, Darnel AD, Moriya T, Kaneko C, et al. Systemic distribution of steroid sulfatase and estrogen sulfotransferase in human adult and fetal tissues. J Clin Endcrinol Metab 2002;87:5760–8.
[23] Ishizuka M, Hatori M, Suzuki T, Miki Y, Darnel AD, Tazawa C, et al. Sex steroid receptors in rheumatoid arthritis. Clin Sci (Lond) 2004;106: 293–300.
[24] Rodan GA, Noda M. Gene expression in osteoblastic cells. Crit Rev Eukaryot Gene Expr 1991;1:85–98.
[25] Ito Y, Miyazono K. RUNX transcription factors as key role of TGF-β superfamily signaling. Curr Opin Genet Dev 2003;13:43–7.
[26] Lønning PE, Geisler J, Krag LE, Erikstein B, Bremnes Y, Hagen AI, et al. Effects of exemestane administered for 2 years versus placebo on bone mineral density, bone biomarkers, and plasma lipids in patients with surgically respected early breast cancer. J Clin Oncol 2005;23:4847–9.
[27] Coombes RC, Hall E, Gibson LJ, Paridaens R, Jassem J, Delozier T, et al. Intergroup Exemestane Study. A randomized trial of exemestane after two to three years of tamoxifen therapy in postmenopausal women with primary breast cancer. N Engl J Med 2004;350:1081–92.
[28] Coleman RE, Banks LM, Girgis SI, Vrdoljak E, Fox J, Porter LS, et al. Skeletal effect of exemestane in the Intergroup Exemestane Study (IES)—2 years bone mineral density (BMD) and bone biomarker data. Breast Cancer Res Treat 2005;94:S233.
[29] Vottero A, Stratalis CA, Ghizzoni L, Longui CA, Karl M, Chrousos GP. Androgen receptor-mediated hypersensitivity to androgen in women with nonhyperandrogenic hirsutism: skewing of X-chromosome inactivation. J Clin Endocrinol Metab 1999;84:1091–5.
[30] Brum IS, Spritzer PM, Paris F, Maturana MA, Audran F, Sultan C. Association between androgen receptor gene CAG repeat polymorphism and plasma testosterone levels in postmenopausal women. J Soc Gynecol Investig 2005;12:135–41.
[31] Vanderschueren D, Vandenput L, Boonen S, Lindberg MK, Bouillon R, Ohlsson C. Androgens and bone. Endocr Rev 2004;25:389–425.
[32] Turner A, Chen T, Barber T, Malabanan A, Holick M, Tangpricha V. Testosterone increases bone mineral density in female-to-male transsexuals: a case series of 15 subjects. Clin Endocrinol (Oxf) 2004;61:560–6.
[33] Ruetsche AG, Kneubuehl R, Birkhaeuser MH, Lippuner K. Cortical and trabecular bone mineral density in transsexuals after long-term cross-sex hormonal treatment: a cross-sectional study. Osteoporos Int 2005;16: 791–98.
[34] Kasperk CH, Wergedal JE, Farley JR, Linkhart TA, Turner RT, Baylink DJ. Androgens directly stimulate proliferation of bone cells in vitro. Endocrinology 1989;124:1576–8.
[35] Kasperk C, Fitzsimmons R, Strong D, Mohan S, Jennings J, Wergedal J, et al. Studies of the mechanism by which androgens enhance mitogenesis and differentiation in bone cells. J Clin Endocrinol Metab 1990;71:1322–9.
[36] Chen Q, Kaji H, Kanatani M, Sugimoto T, Chihara K. Testosterone increases osteoprotegerin mRNA expression in mouse osteoblast cells. Horm Metab Res 2004;36:674–8.
[37] Bord S, Horner A, Beavan S, Compston J. Estrogen receptors alpha and beta are differentially expressed in developing human bone. J Clin Endocrinol Metab 2001;86:2309–14.
[38] Sala A, Watson R. B-Myb protein in cellular proliferation, transcription control, and cancer: latest developments. J Cell Physiol 1999;179:245–50.
[39] Chalhoub N, Benachenhou N, Rajapurohitam V, Pata M, Ferron M, Frattini A, et al. Grey-lethal mutation induces severe malignant autosomal recessive osteopetrosis in mouse and human. Nat Med 2003;9:399–406.
[40] Boulet AM, Capecchi MR. Multiple roles of Hoxa11 and Hoxd11 in the formation of the mammalian forelimb zeugopod. Development 2004; 131:299–309.
[41] Lundberg P, Lundgren I, Mukohyama H, Lehenkari PP, Horton MA, Lerner UH. Vasoactive intestinal peptide (VIP)/pituitary adenylate cyclase-activating peptide receptor subtypes in mouse calvarial osteoblasts: presence of VIP-2 receptors and differentiation-induced expression of VIP-1 receptors. Endocrinology 2001;142:339–47.
[42] Gutierrez J, Osses N, Brandan E. Changes in secreted and cell associated proteoglycan synthesis during conversion of myoblasts to osteoblasts in response to bone morphogenetic protein-2: role of decorin in cell response to BMP-2. J Cell Physiol 2006;206:58–67.
[43] Omi M, Fisher M, Maihle NJ, Dealy CN. Studies on epidermal growth factor receptor signaling in vertebrate limb patterning. Dev Dyn 2005;233:288–300.
[44] Rodan GA, Raisz LG, Bilezikian JP. Pathophysiology of osteoporosis. . (chapter 73)In: Bilezikian JP, Raisz LG, Rodan GA, editors. Principles of bone biology, 2nd ed., vol. 1. NY, USA: Academic Press, A division of Harcourt, Inc.; 2002. p. 1275–90.
[45] Kellinsalmi M, Monkkonen H, Monkkonen J, Leskela HV, Parikka V, Hamalainen M, et al. In vitro comparison of clodronate, pamidronate and zoledronic acid effects on rat osteoclasts and human stem cell-derived osteoblasts. Basic Clin Pharmacol Toxicol 2005;97:382–91.
[46] Chen Q, Kaji H, Sugimoto T, Chihara K. Testosterone inhibits osteoclast formation stimulated by parathyroid hormone through androgen receptor. FEBS Lett 2001;491:91–3.
[47] Abu EO, Horner A, Kusec V, Triffitt JT, Compston JE. The localization of androgen receptors in human bone. J Clin Endocrinol Metab 1997; 82:3493–7.
[48] Wiren KM, Orwoll ES. Androgens: receptor expression and steroid action in bone. . (chapter 43)In: Bilezikian JP, Raisz LG, Rodan GA, editors. Principles of bone biology, 2nd ed., vol. 1. NY, USA: Academic Press, A division of Harcourt, Inc.; 2002. p. 757–72.
[49] Chow LW, Wong JL, Toi M. Celecoxib anti-aromatase neoadjuvant (CAAN) trial for locally advanced breast cancer: preliminary report. J Steroid Biochem Mol Biol 2003;86:443–7.
[50] Sato T, Morita I, Sakaguchi K, Nakahama KI, Smith WL, Dewitt DL, et al. Involvement of prostaglandin endoperoxide H synthase-2 in osteoclast-like cell formation induced by interleukin-1 beta. J Bone Miner Res 1996;11:392–400.